JOURNAL OF GEOPHYSICAL RESEARCH, VOL. 95, NO. D7, PAGES 10,205–10,233, JUNE 20, 1990

Aircraft Measurements of NO_x Over the Eastern Pacific and Continental United States and Implications for Ozone Production

M. A. CARROLL,[1] D. R. HASTIE,[2] B. A. RIDLEY,[3] M. O. RODGERS,[4] A. L. TORRES,[5] D. D. DAVIS,[4] J. D. BRADSHAW,[4] S. T. SANDHOLM,[4] H. I. SCHIFF,[2] D. R. KARECKI,[6] G. W. HARRIS,[6] G. I. MACKAY,[6] G. L. GREGORY,[7] E. P. CONDON,[8] M. TRAINER,[1,9] G. HUBLER[1,9] D. D. MONTZKA,[1,9] S. MADRONICH,[3] D. L. ALBRITTON,[1] H. B. SINGH,[8] S. M. BECK,[7] M. C. SHIPHAM,[7] AND A. S. BACHMEIER[7]

Measurements of NO, NO_2, O_3, and CO are presented from 13 aircraft flights made over the eastern Pacific Ocean and the continental United States in August and September 1986 during the NASA GTE/CITE 2 program. Measurements of NO by three different groups (two different techniques) and of NO_2 by three different groups (three different techniques) are presented and examined along with calculated NO_x ($NO + NO_2$) for correlations with O_3, CO, and dew-point temperature (DPT) primarily as a function of air mass category. Median values of NO and NO_2 in the marine boundary layer were 4.0 and 10.4 pptv, respectively, and 12.4 and 18.0 pptv in the marine free troposphere. In the continental boundary layer, median values of NO and NO_2 were 34.5 and 75.0 pptv, respectively, and 13.0 and 36.0 pptv at altitudes above 3 km in air masses having continental influence. In the maritime NO_x data set a negative correlation is often observed between NO_x and DPT, while positive correlations were typically observed between NO_x and O_3 and between NO_x and CO. As expected, then, negative correlations were often observed between O_3 and DPT and between CO and DPT, along with positive correlations between CO and O_3. In the continental data set, positive correla- tions were typically observed between NO_x and DPT, O_3, and CO. Additionally, the various air masses were examined with respect to regions of net ozone production or net ozone destruction. In all but one case in the marine boundary layer, model calculations indicate that there is significant ozone destruction. In the continental boundary layer, however, calculations indicate significant ozone production. In the middle free troposphere at 5 ± 1 km, the in situ ozone formation was most often nearly in balance with ozone destruction.

[1]Aeronomy Laboratory, National Oceanic and Atmospheric Administration, Aeronomy Laboratory, Boulder, Colorado.
[2]Chemistry Department, York University, Downsview, Ontario, Canada.
[3]National Center for Atmospheric Research, Boulder, Colorado.
[4]School of Geophysical Sciences, Georgia Institute of Technology, Atlanta.
[5]NASA Goddard Space Flight Center, Wallops Flight Facility, Wallops Island, Virginia.
[6]Unisearch Associates, Concord, Ontario, Canada.
[7]NASA Langley Research Center, Hampton, Virginia.
[8]NASA Ames Research Center, Moffett Field, California.
[9]Cooperative Institute for Research in Environmental Sciences, University of Colorado, Boulder.

Paper number 89JD02939.
0148-0227/90/89JD-02939$05.00

INTRODUCTION

Nitric oxide (NO) and nitrogen dioxide (NO_2) play a critical role in determining tropospheric levels of ozone (O_3) [*Crutzen*, 1974; *Chameides and Walker*, 1973, 1976; *Chameides and Stedman*, 1977; *Chameides*, 1978; *Fishman and Crutzen*, 1977, 1978; *Liu*, 1977; *Fishman et al.*, 1979*a*, *b*; *Liu et al.*, 1980, 1983; *Logan et al.*, 1981; *Logan*, 1983, 1985; *Dignon and Hameed*, 1985]. Because O_3 is a radiatively important trace species and its photodissociation leads to the formation of hydroxyl in the troposphere, NO and NO_2 play an indirect role in the global radiation budget and indirectly influence the lifetimes and abundances of many reactive species in the troposphere.

The observations reported here were made during August and September of 1986 as part of the NASA Global Tropospheric Experiment, Chemical Instrumentation Test and Evaluation program (GTE/CITE 2), outlined by *Hoell et al.* [this issue]. Measurements of the major daytime

reactive nitrogen species (NO and NO_2), nitric acid (HNO_3) [*Huebert et al.*, this issue; *LeBel et al.*, this issue; *Gregory et al.*, this issue (*c*)], peroxyacetyl nitrate (PAN) [*Ridley et al.*, this issue; *Singh et al.*, this issue; *Gregory et al.*, this issue (*d*)], and total odd-nitrogen (NO_y) [G. Hübler et al., unpublished material, 1990] were made on board the NASA Wallops Flight Center's Electra aircraft. Four groups participated in the measurements and intercomparison effort focused on the NO_x species (NO_x = NO + NO_2). The results of the intercomparisons are discussed by *Gregory et al.* [this issue (*a*, *b*)], and detailed comparisons of observed ratios of NO_2 to NO with theoretical calculations are the subject of manuscripts by *Chameides et al.* [this issue] and M.A. Carroll et al., (unpublished material, 1990). This paper focuses on the distribution of the NO_x species (including boundary layer/free troposphere and marine/continental contrasts), the correlations between the NO_x species and O_3, CO, and dew-point temperature (DPT), and a survey of the data with respect to regions of net ozone production or loss.

EXPERIMENTAL

As mentioned above, four different groups conducted measurements of the NO_x species. The techniques employed included tunable diode laser absorption for the measurement of NO_2 (York, investigators at York University) [*Schiff et al.*, this issue], photo-fragmentation/two-photon laser-induced fluorescence for the simultaneous measurement of NO_2 and NO (GIT, investigators at the Georgia Institute of Technology) [*Sandholm et al.*, this issue], chemiluminescence/ferrous sulfate conversion for the serial measurement of NO and NO_2 (WFF, an investigator at NASA Wallops Flight Facility), and chemiluminescence/photolytic conversion for simultaneous measurements of NO and NO_2 (NOCAR, investigators at the National Center for Atmospheric Research and the National Oceanic and Atmospheric Administration) [*Ridley et al.*, 1988*a*]. Data from WFF and NOCAR are typically presented as 1-min averages, York data as 150-s averages, and GIT data as 2-min averages for NO and as averages over 6 or 10 min for NO_2 (except in the case of flight 9, where 2-min averages are presented). Although the reader is referred to *Gregory et al.*, [this issue (*a*, *b*)] for a detailed account of instrument capabilities and appropriate references, it is important to keep in mind that the detection limits of the various techniques differ. Briefly, for a 1-min average for NO, the WFF technique has a 2σ detection limit of 4 pptv and a 2σ precision value of $\pm$ 4 pptv + 6%, or ~ $\pm$ 5 pptv for most of the measurements made during CITE 2. The GIT technique has a 2σ detection limit of 2.5 pptv NO with a 2σ precision value of $\pm$7 pptv for a 2-min average for a conentration tenfold above the detection limit (where both limit of detection and measurement precision scale with the inverse square root of the integration time). The NOCAR technique has a 2σ detection limit of 2 pptv NO and a 2σ precision value of $\pm$3 pptv for a 1-min average. As discussed by *Gregory et al.*, [this issue (*b*)], the detection limit for the York technique was estimated to be about 25 pptv NO_2 based on laboratory tests. Detection limits varied slightly depending on the sampling environment. The total uncertainty for mixing ratios well above the 25-pptv detection limit (e.g., 100 pptv) was estimated at 25%. At 50 pptv NO_2 the total uncertainty was of the order of 45%. The NOCAR technique has a 2σ detection limit of 9 pptv and a 2σ precision value of $\pm$10 pptv for a 1-min average of NO_2. For the 6-min running averages of NO_2 the GIT technique has a 2σ detection limit of 14 pptv with a 2σ precision value of $\pm$15 pptv for a concentration fivefold above the detection limit. Again, the detection limit and measurement precision scale with the inverse square root of the integration time, resulting in a 2σ detection limit of 11 pptv with a 2σ precision value of $\pm$12 pptv for the 10-min running averages of NO_2. These values for detection limits and precision for GIT NO_2 assume an NO_2/NO ratio of unity. It should be noted that the York instrument was configured to measure nitric acid on flights 10, 11, 15, and 16; thus no NO_2 data are available for these flights. Additionally, as in other recent intercomparisons, the ferrous sulfate converter was found to convert PAN to NO, resulting in NO_2 values significantly higher (3-10 times) than those reported by the other techniques [*Gregory et al.*, this issue (*b*); *Ridley et al.*, 1988*b*; *Fehsenfeld et al.*, 1990]. Thus the WFF NO_2 data have not been included in this discussion.

As the NO_x to NO_y ratio will be discussed briefly later on, it is appropriate to comment on the NO_y measurement technique here. Total reactive odd nitrogen was measured by converting the NO_y subspecies catalytically on a heated Au surface to NO. The resulting NO was quantified with an NO/O_3 chemiluminescence detector [G. Hübler et al., (unpublished material, 1990)].

OBSERVATIONS

This series of 16 flights began with three test flights out of Wallops Island, Virginia. To facilitate the reader's referring to other manuscripts in this issue, we adopt the same numbering system in discussing the 13 official program flights (numbered 4-16). Several of the primary goals of the flight series required clean air measurements, and thus nine of the 13 flights were based out of NASA's Ames Research Center, Moffett Field, California, for ease in access to air masses over the Pacific Ocean. Flights 6, 7, 8, 10, and 12 were made over the eastern Pacific Ocean, flights 9, 11, 13, and 14 were conducted over the southwestern continental United States, and flights 4, 5, 15, and 16 were transit flight sets from the east-to-west and the west-to-east coasts, respectively. For discussion, the data have been divided into two broad air mass categories, maritime and continental. Within these two categories there are subcategories according to air mass origin as determined by 60-hour back-trajectory analyses [*Shipham et al.*, this issue] and altitude.

Marine air masses encountered include maritime polar (mp) and maritime tropical (mt) and are named to reflect the

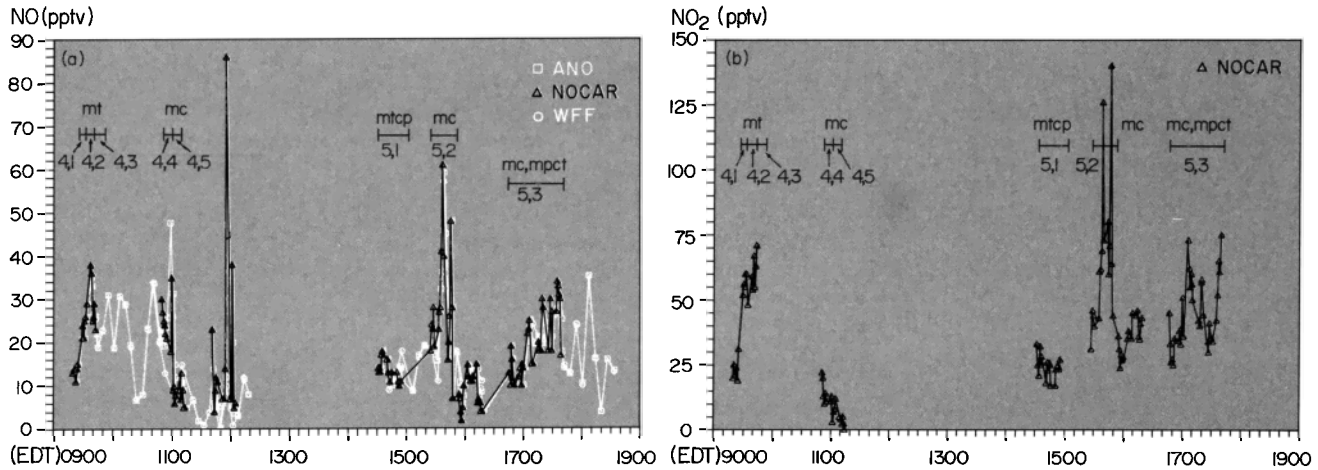

Plate 1. August 11 trace species measurements: (*a*) NO mixing ratios and (*b*) NO_2 mixing ratios.

origin. Continental air masses encountered include continental polar (cp) and continental tropical (ct), similarly named. Mixtures of these air masses were also encountered, including mixed maritime (mm), mixed maritime and continental tropical (mmct), maritime tropical and continental polar (mtcp), and maritime polar and continental tropical (mpct). Air masses of continental origin having no maritime influence for the past 60 hours (but not distinguished as either cp or ct) are labeled mixed continental (mc).

The NO and NO_2 measurements as made by each group are presented for each flight or set of flights in Plates 1-11. Included for an examination of trends and variations among the trace species are measurements of O_3, CO, temperature (T), DPT, flight altitude, and ground elevation (continental data) in Figures 1-11. In situ measurements of O_3 were obtained by G. Gregory, NASA Langley Research Center, via chemiluminescent detection. CO measurements were made by E. Condon, NASA Ames Research Center by grab sample followed either by ground-based gas chromatographic analysis or by real time analysis via a mercuric oxide reduction gas detector [*Singh et al.*, this issue]. The Electra was equipped with instrumentation to measure T, DPT, altitude, latitude, longitude, true air speed, wind speed, wind direction, and radiation, and these measurements were provided by support personnel at NASA Langley Research Center. A software routine was used to generate values of ground elevation from the aircraft measurements of latitude and longitude. O_3, CO, T, DPT, altitude, and ground elevation are reported in Figures 1-11 as 1-min averages except for CO (instantaneous grab samples obtained approximately every 15 min). In Plates and Figures 1-11, the NO and NO_2 levels are in pptv, O_3 and CO levels are in ppbv, temperature (SAT) and dew point (DPT) are given in degrees Celsius, altitude and ground elevation are in kft (1 kft = 0.3048 km), and the abscissas are local time. Ave refers to data from the average data set generated as described below. Instances where ave NO or ave NO_2 appear to exceed the other values are due to a choice of ordinate to show most of the data; other points are off-scale. Possible correlations among the observations were examined via linear regression analyses,

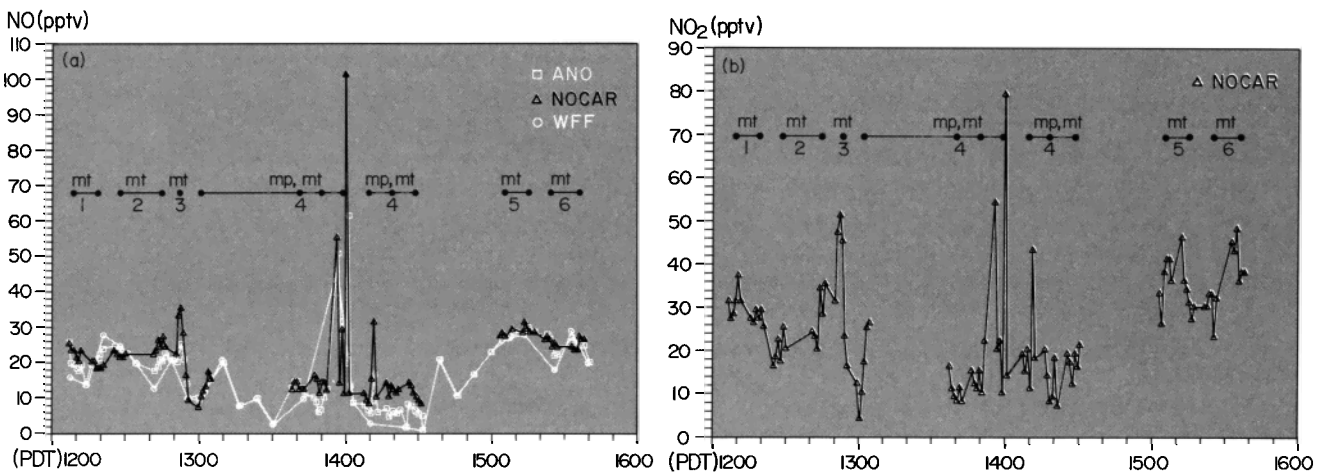

Plate 2. August 15 trace species measurements: (*a*) NO mixing ratios and (*b*) NO_2 mixing ratios.

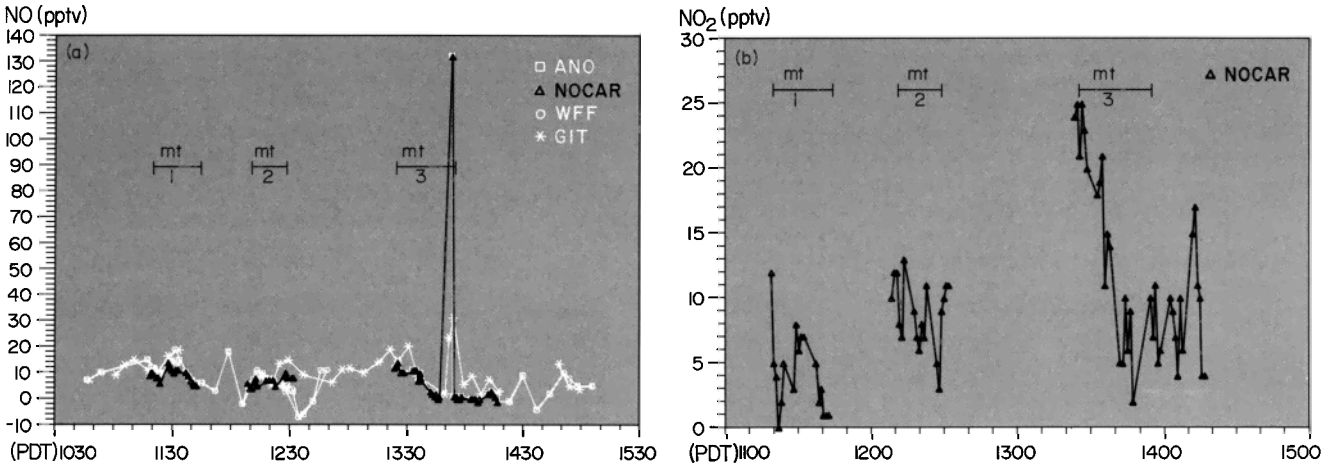

Plate 3. August 19 trace species measurements: (*a*) NO mixing ratios and (*b*) NO_2 mixing ratios.

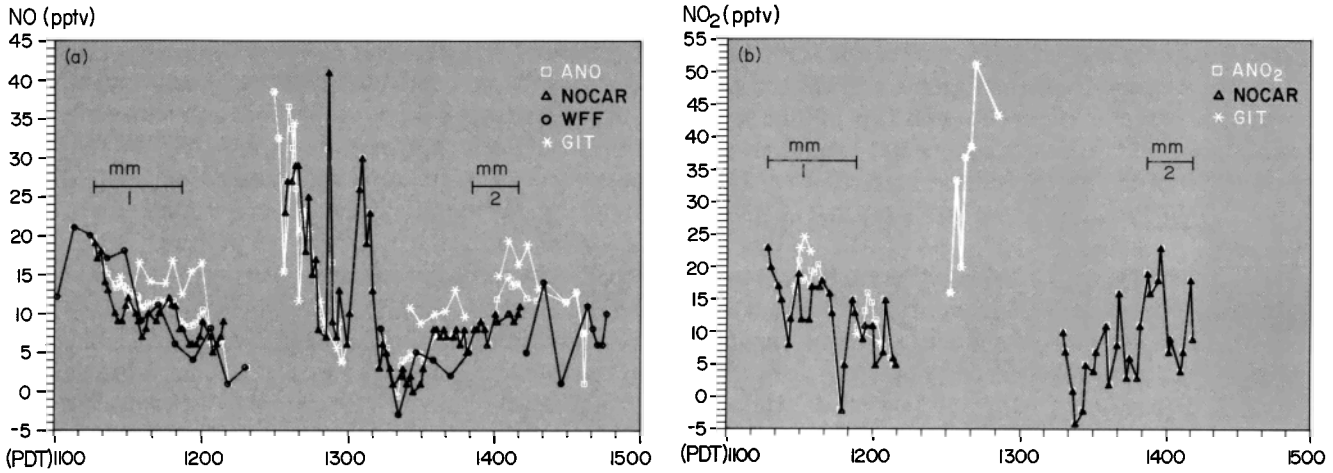

Plate 4. August 21 trace species measurements: (*a*) NO mixing ratios and (*b*) NO_2 mixing ratios.

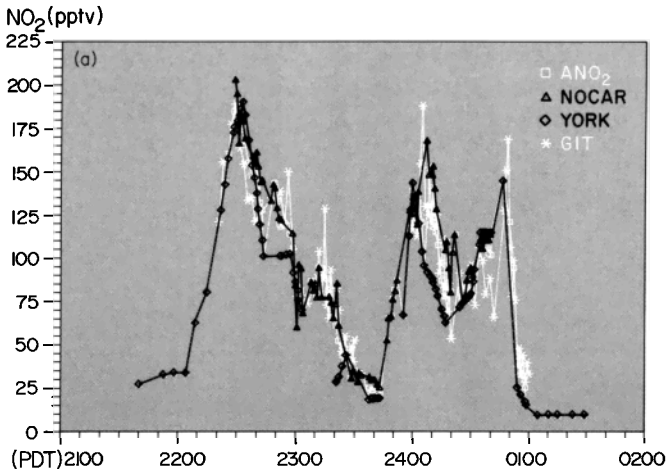

Plate 5. August 23-24 trace species measurements for NO_2 mixing ratios.

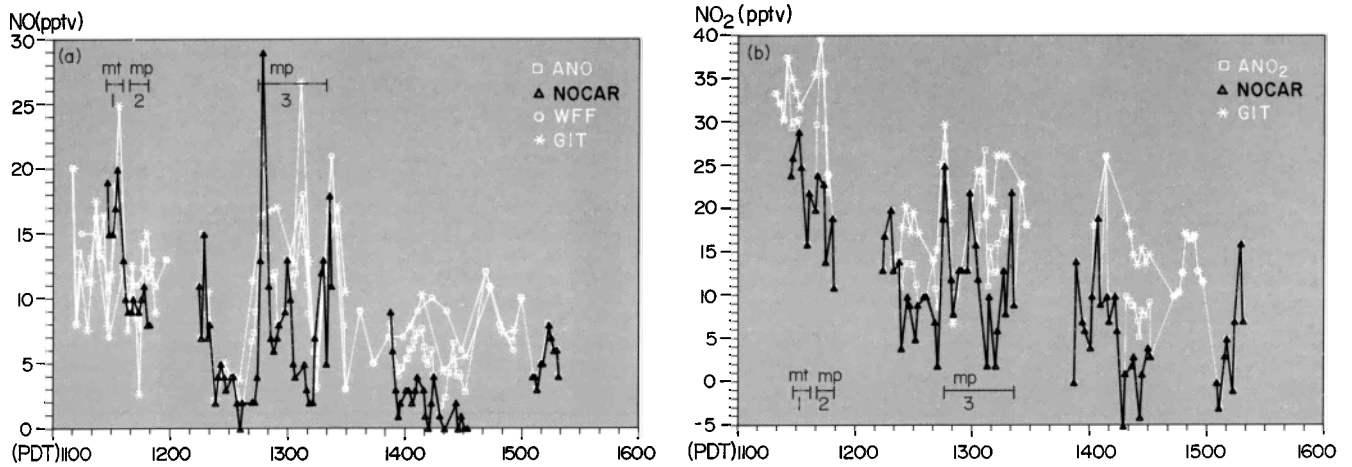

Plate 6. August 26 trace species measurements: (*a*) NO mixing ratios and (*b*) NO_2 mixing ratios.

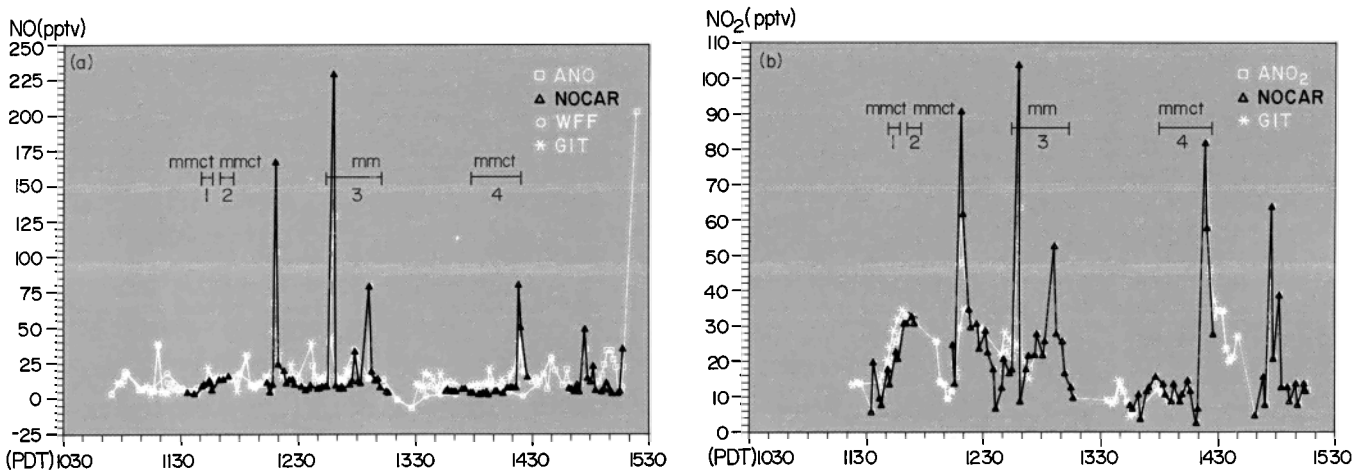

Plate 7. August 28 trace species measurements: (*a*) NO mixing ratios and (*b*) NO_2 mixing ratios.

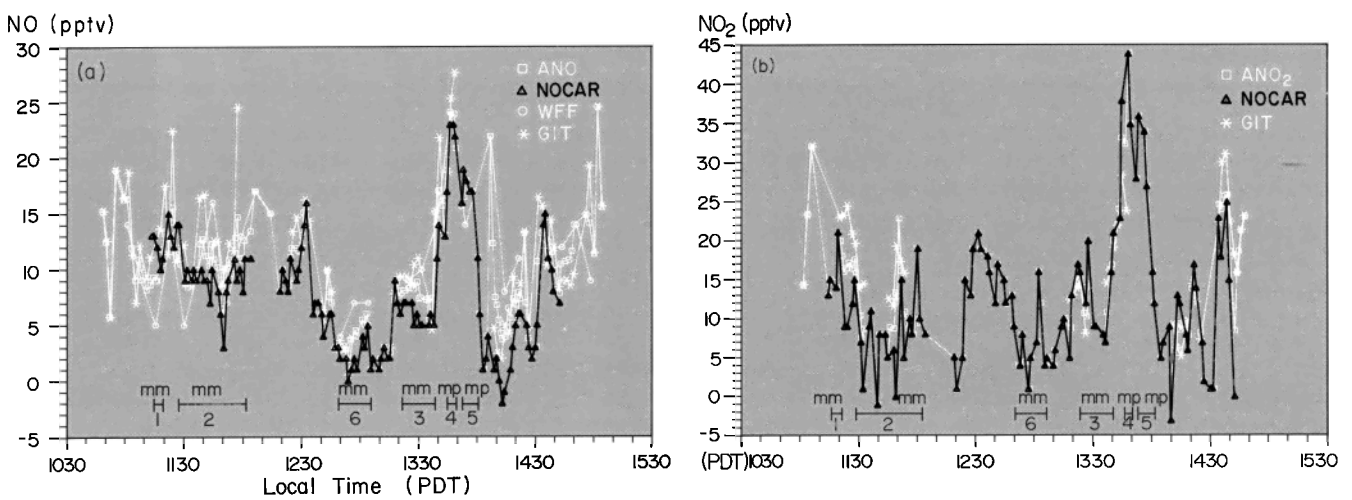

Plate 8. August 30 trace species measurements: (*a*) NO mixing ratios and (*b*) NO_2 mixing ratios.

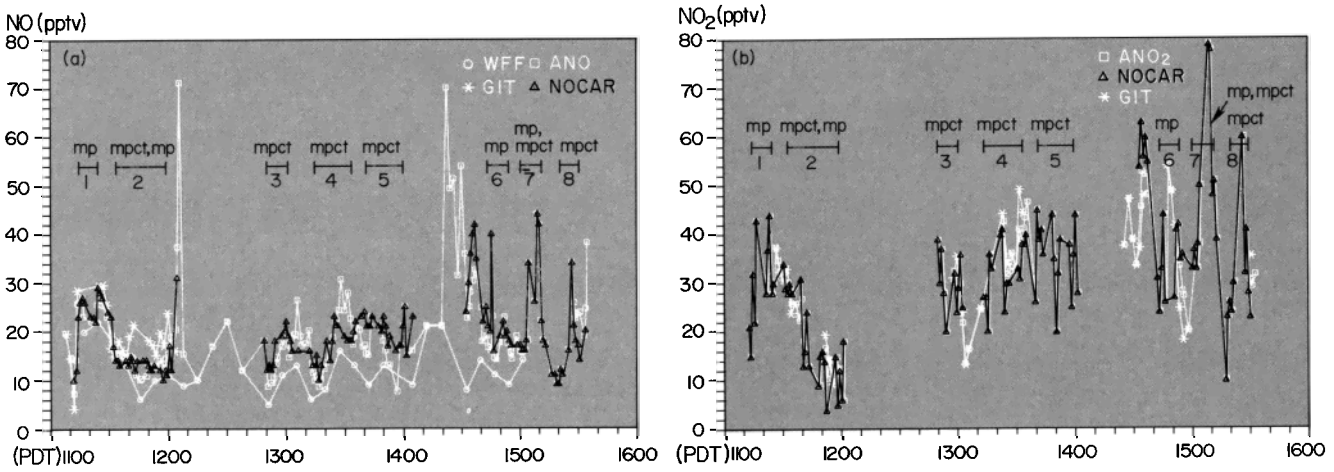

Plate 9. August 31 trace species measurements: (*a*) NO mixing ratios and (*b*) NO_2 mixing ratios.

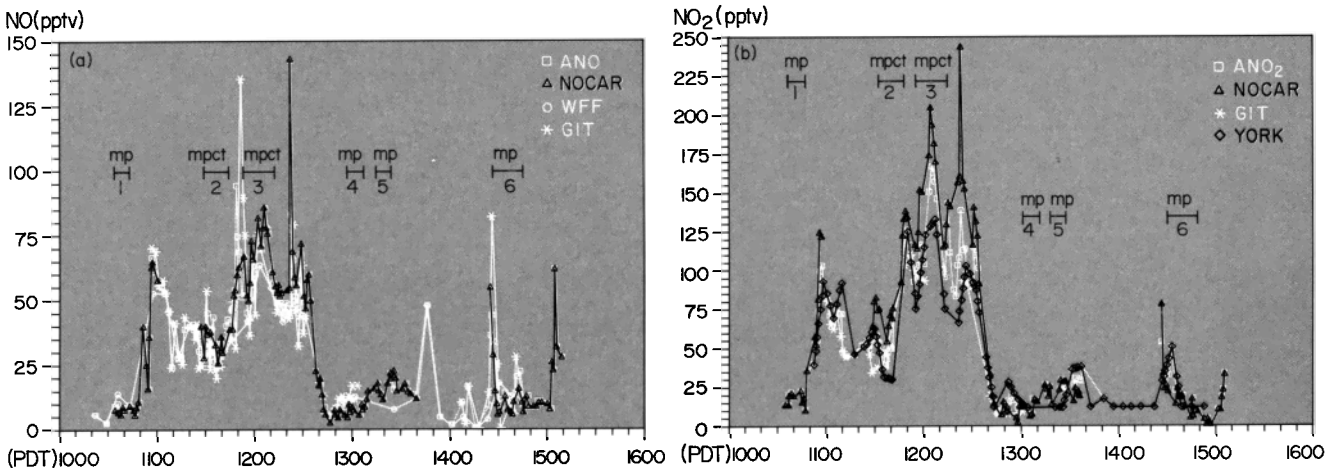

Plate 10. September 2 trace species measurements: (*a*) NO mixing ratios and (*b*) NO_2 mixing ratios.

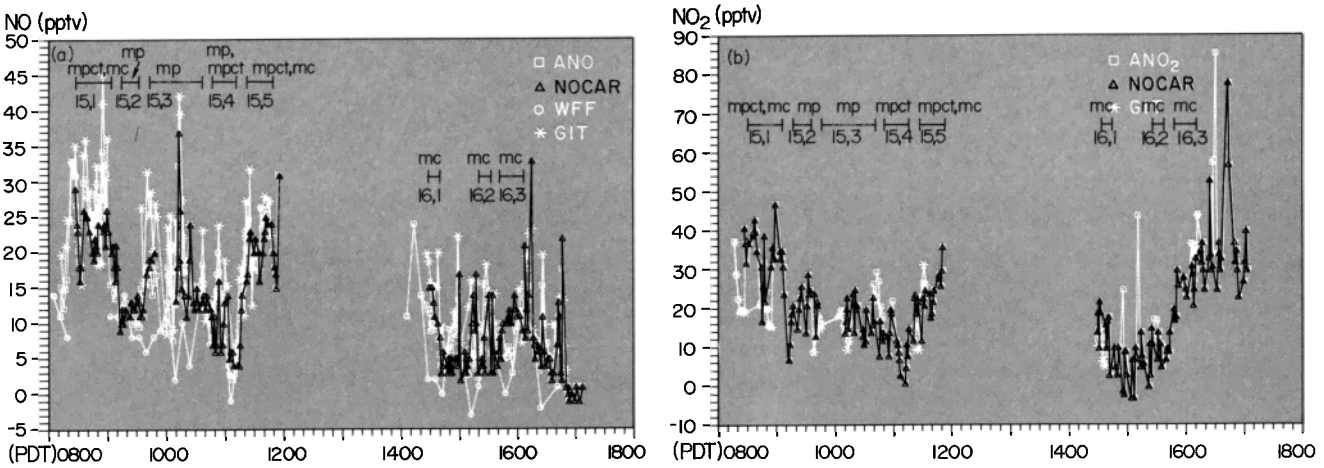

Plate 11. September 5 trace species measurements: (*a*) NO mixing ratios and (*b*) NO_2 mixing ratios.

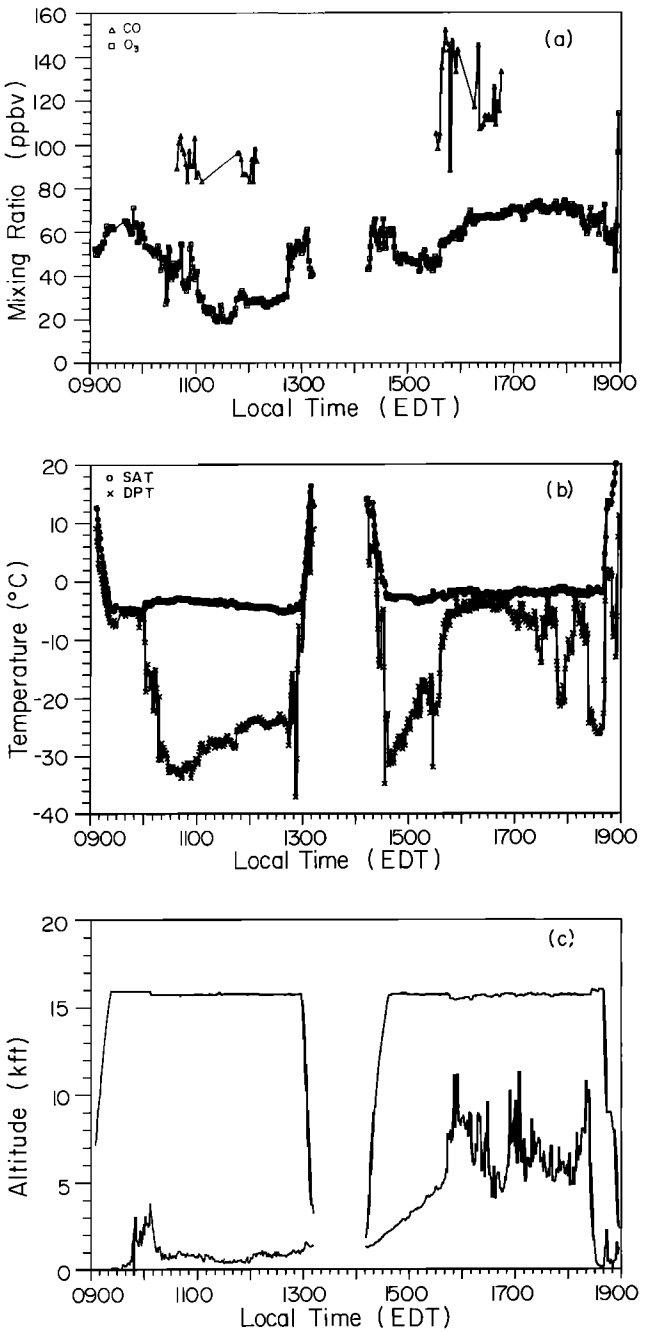

Fig. 1. August 11 trace species measurements: (*a*) O_3 and CO mixing ratios, (*b*) SAT and DPT, and (*c*) aircraft altitude and ground elevation.

and the results were tabulated according to air mass category and altitude. Additionally, the ambient values of CO, O_3, NO, and nonmethane hydrocarbons (NMHCs), T, and DPT used in our model analyses to calculate net ozone production or destruction ($P(O_3)$) are listed in Table 1 along with local time, air mass category, ambient NO_2, and calculated $P(O_3)$. NMHC measurements (approximately 10 grab samples were collected per flight) were made by H. Singh, NASA Ames Research Center, using ground-based gas chromatographic analysis and included ethane, propane, ethylene, and propylene, as listed in Table 1. A further discussion of these measurements is presented by *Singh et al.*, [this issue]. Model analyses were typically conducted for periods when the NO_x species were relatively constant, and the time periods chosen are listed in Table 1 and are represented by horizontal bars in the NO and NO_2 plots in Plates 1-11 with the model run number and air mass category noted.

The figures containing the NO and NO_2 data also display the results of the data analysis performed by *Hastie et al.* [1987] that created an average data set for each species. The individual investigators' data sets were averaged to improve the precision of the measurements. In addition, analysis of the spread of the simultaneously obtained data from the different groups was useful in assessing its suitability for addressing the scientific questions in this and other papers.

The data were preselected to account for known discrepancies as indentified in the NO_2 intercomparison [*Gregory et al.*, this issue (*b*)]. The WFF NO_2 data were not included. There was a disagreement between NOCAR and York in flight 4, and since there was a discontinuity in the York data between flights 4 and 5, neither York data set was included. In addition, the intercomparison pointed to a bias in the York data below 50 pptv, and so such data were also excluded. GIT performed a number of tests on their first full flight (7) so these data were also excluded.

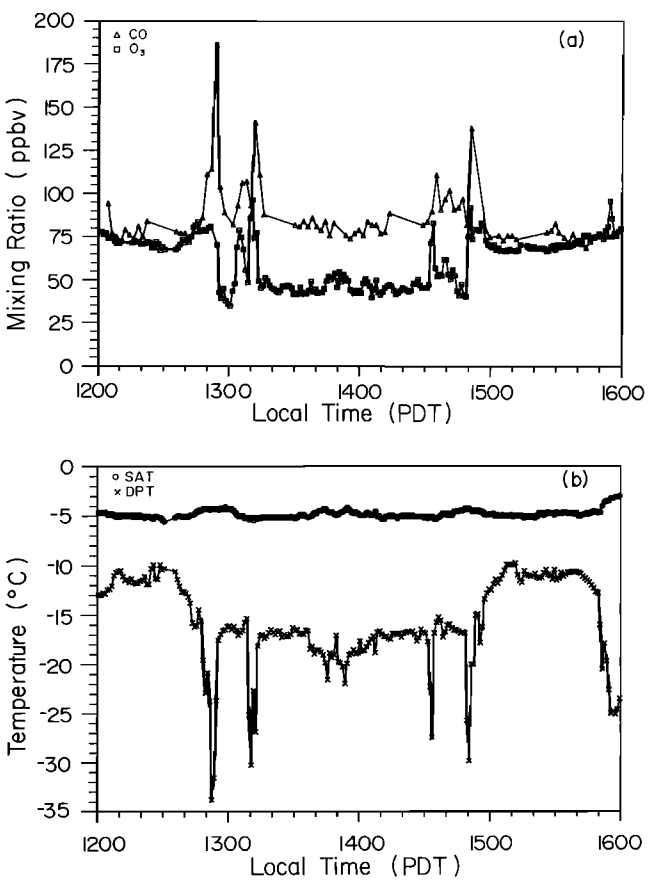

Fig. 2. August 15 trace species measurements: (*a*) O_3 and CO mixing ratios, and (*b*) SAT and DPT.

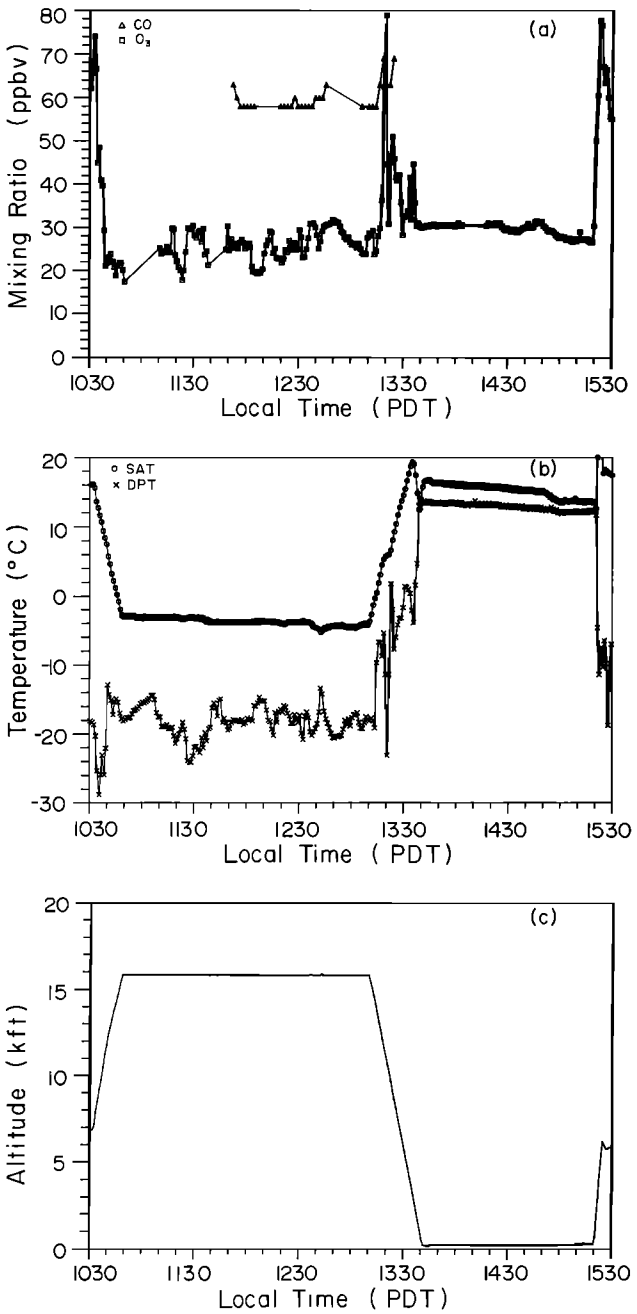

Fig. 3. August 19 trace species measurements: (*a*) O_3 and CO mixing ratios, (*b*) SAT and DPT, and (*c*) aircraft altitude.

All remaining NO_2 and NO data were combined into average NO_2 and NO data as follows. All data were transformed to 1-min averages. This required no changes to the NOCAR NO_2 or NO data or the WFF NO data. The GIT 6-min running average NO_2 and NO and the York 150-s averaged NO_2 were interpolated to match the 1-min average. The York data were interpolated over the frequent 150-s zeros, but interpolation was not carried out over any other zero or calibration cycles. This interpolation procedure could introduce errors if the concentration were changing in the time periods over which the data were averaged; however, the area over which the measurements were made proved sufficiently homogenous that this was not a problem, except when the aircraft was ascending or descending.

Once these instrument specific 1-min averages were generated, they were averaged to give the mean NO_2 or NO for that 1-min interval. These values were then added to generate the average NO_x concentration. To estimate the reliability of these values, the standard deviation of the NO and NO_2 averages were propagated to give a multi-instrument uncertainty. This uncertainty was occasionally as high as 100% but was more generally of the order of 40%, which gave us the confidence to use the data to address the scientific questions.

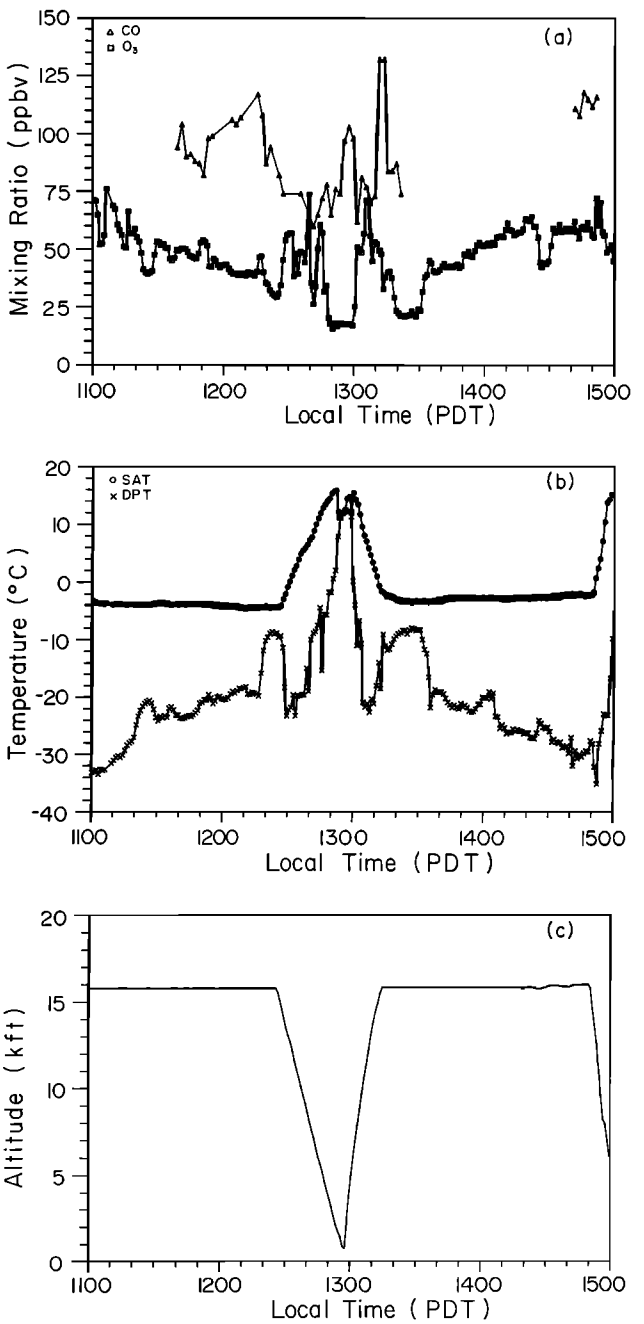

Fig. 4. August 21 trace species measurements: (*a*) O_3 and CO mixing ratios, (*b*) SAT and DPT, and (*c*) aircraft altitude.

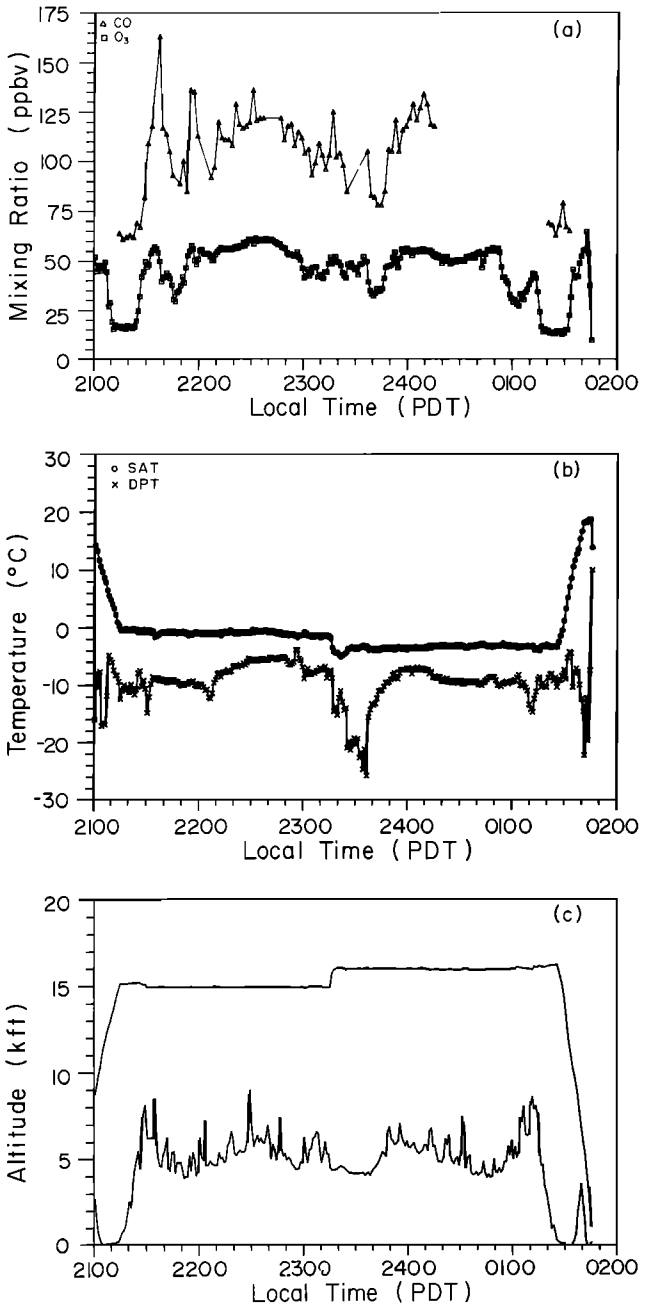

Fig. 5. August 23-24 trace species measurements: (*a*) O_3 and CO mixing ratios, (*b*) SAT and DPT, and (*c*) aircraft altitude and ground elevation.

NO AND NO_2 MEASUREMENTS

Flights 4 and 5 were transit flights conducted on August 11, 1986, from Wallops Island, Virginia, to Moffett Field, California, with a stop at McConnell Air Force Base in Kansas, and are discussed here as a set. The mixing ratios of NO and NO_2 are presented in Plate 1*a* and 1*b*, while traces of CO and O_3 are presented in Figure 1*a*, static air temperature (SAT) and DPT are shown in Figure 1*b*, and aircraft altitude and ground elevation are shown in Figure 1*c*. During these flights we see changes in the NO_x species with var- iations in air mass type. For example, an mt air mass was encountered at the start of flight 4 with NO mixing ratios of about 25 pptv until 1000 (EDT), when the air mass category changed to mc, bringing a drop to about 10 pptv NO. A similar change is observed in the O_3 mixing ratios where the transition to cooler, drier continental air (northwest flow originating over southwest Canada, [see *Shipham et al.*, this issue]) brought a drop in O_3 from 50-60 ppbv to 20-30 ppbv. Additionally, the impact of convection as the flight path crossed the Rocky Mountains (see Figure 1*c*) is seen in the variability and the elevated values of the NO_x species after 1500 (EDT), likely indicative of boundary layer air mixing aloft.

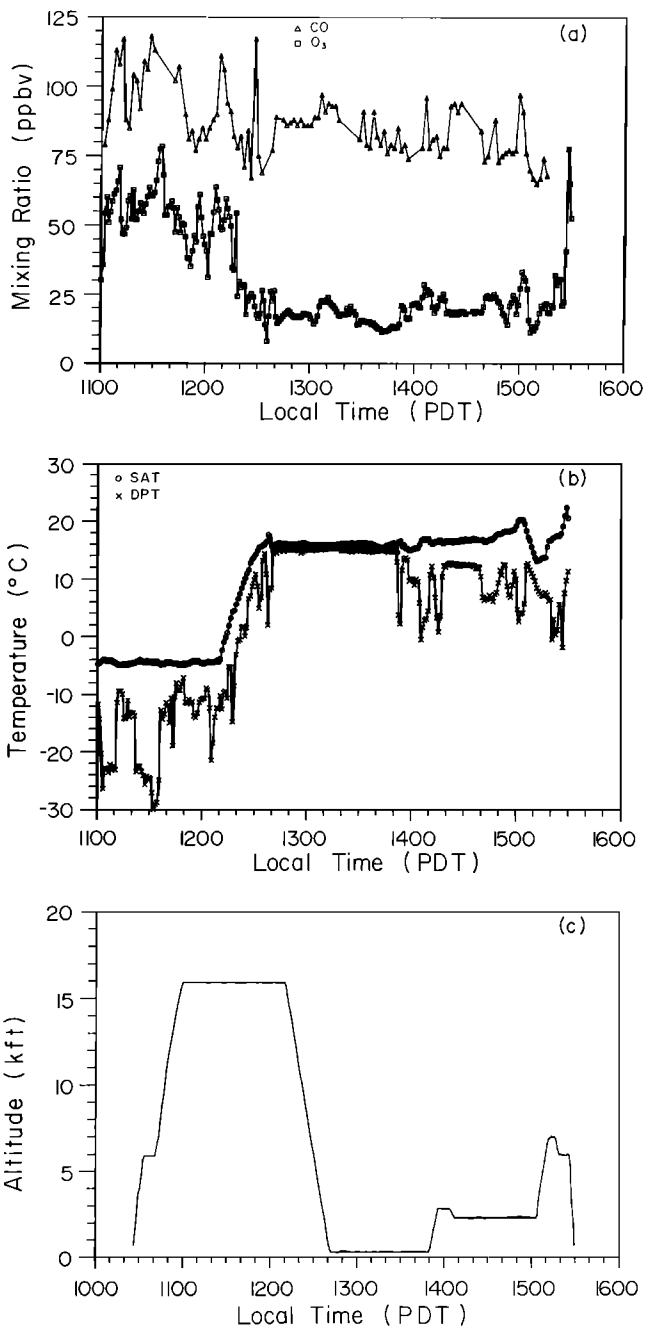

Fig. 6. August 26 trace species measurements: (*a*) O_3 and CO mixing ratios, (*b*) SAT and DPT, and (*c*) aircraft altitude.

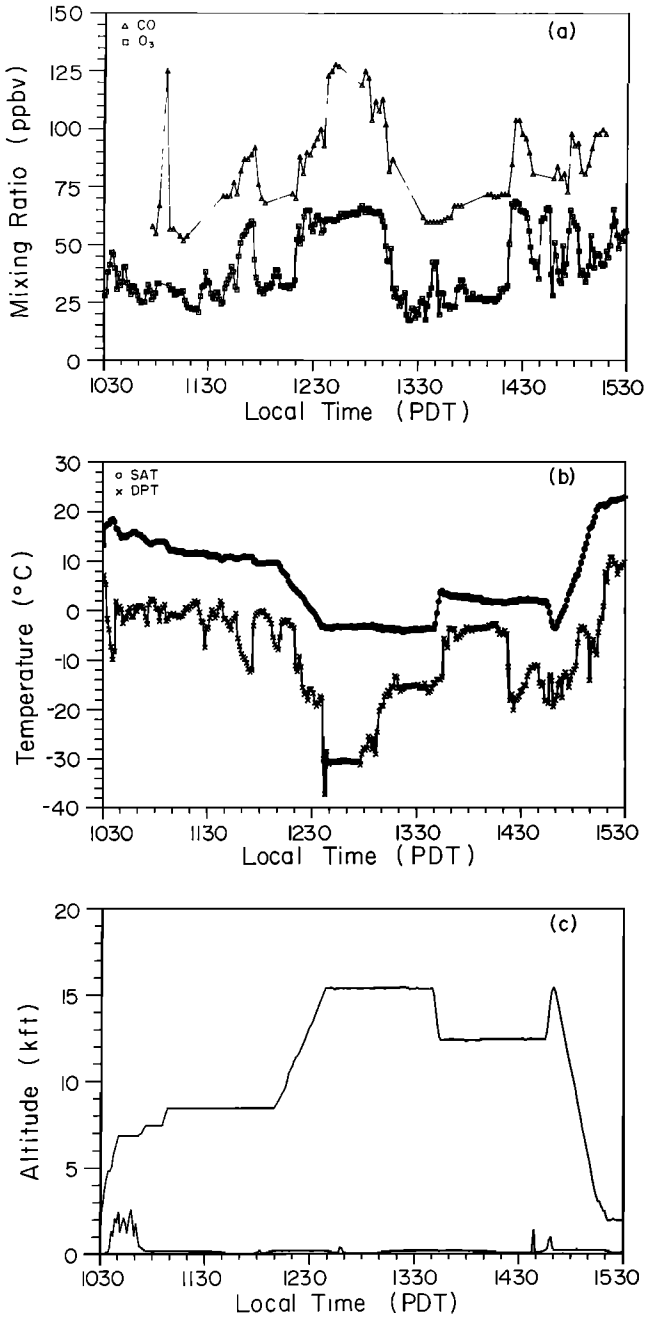

Fig. 7. August 28 trace species measurements: (*a*) O_3 and CO mixing ratios, (*b*) SAT and DPT, and (*c*) aircraft altitude and ground elevation.

Flight 6 was conducted on August 15, 1986. The flight was made at a constant altitude of 4.9 km (16 kft) over the Pacific Ocean. The symmetry of the flight path is evident in the mixing ratio and temperature traces shown in Plates 2*a* and 2*b* and Figures 2*a* and 2*b*. The air mass encountered was predominently mt, with a brief period of mp air encountered near the turnaround point. Within the mt air mass, however, two different environments were encountered, coinciding with the presence or absence of a thick cloud deck well below the aircraft which was present on the initial out-bound leg as seen in the data traces from 1200 to 1300 (PDT) and on the return after ~ 1500 (PDT). The NO_x, O_3, and DPT traces reflect these two environments with significantly lower values observed in clear air, 1300-1500 (PDT). The enhancements observed in the NO_x species near 1400 (PDT) are the result of encountering our own exhaust after turning around.

Flight 7 was conducted on August 19, 1986, and was a multilevel flight over the Pacific Ocean. The mixing ratios of NO and NO_2 are presented in Plates 3*a* and 3*b*, while traces of CO and O_3 and SAT and DPT are presented in Figures 3*a* and 3*b*, with aircraft altitude shown in Figure

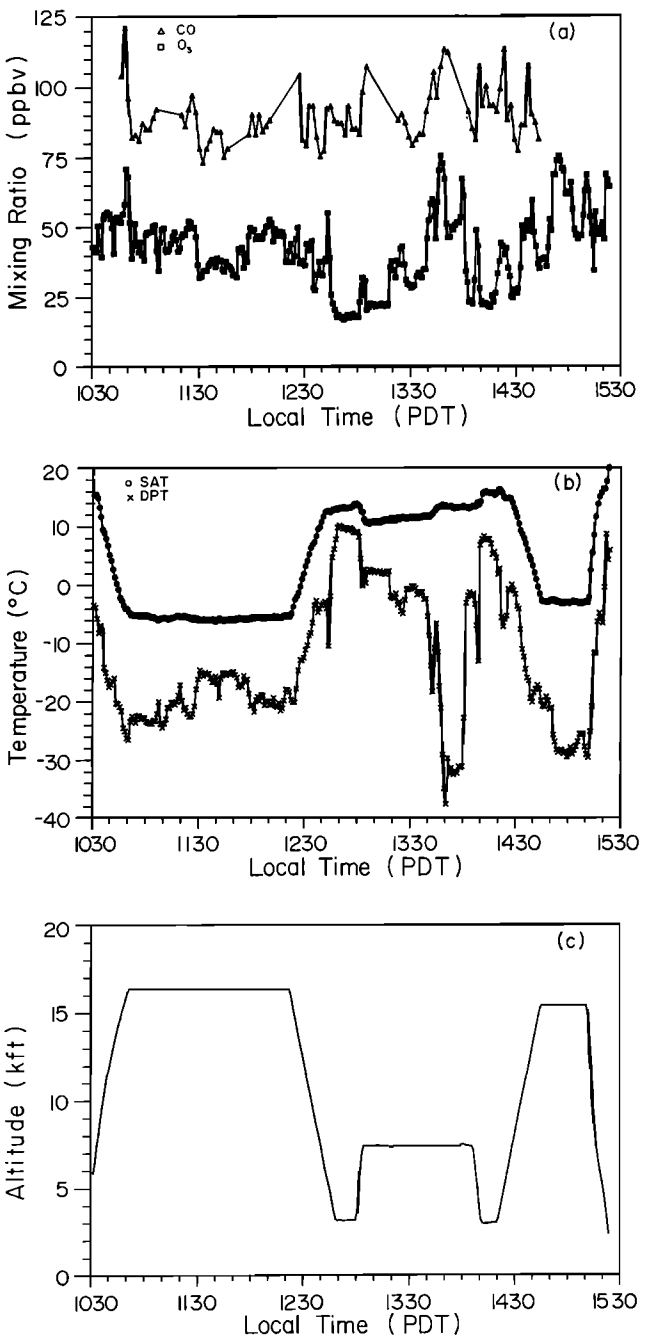

Fig. 8. August 30 trace species measurements: (*a*) O_3 and CO mixing ratios, (*b*) SAT and DPT, and (*c*) aircraft altitude.

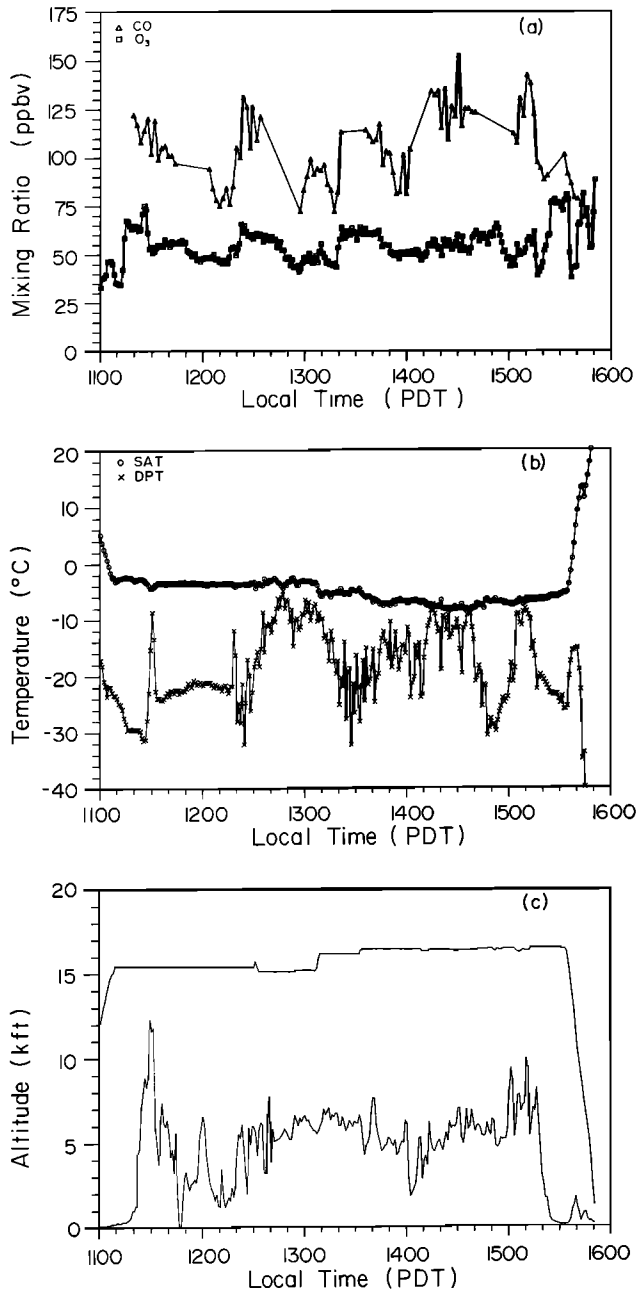

Fig. 9. August 31 trace species measurements: (*a*) O_3 and CO mixing ratios, (*b*) SAT and DPT, and (*c*) aircraft altitude and ground elevation.

3*c*. As in Flight 6, the air mass encountered was mt with observations made in the free troposphere during the first part of the flight (1100-1300 PDT) followed by observations made in the marine boundary layer from 1340 to 1520 PDT. The NO_x and O_3 mixing ratios reflect pristine air conditions throughout this flight with O_3 mixing ratios of 20-30 ppbv and NO_x mixing ratios averaging only 14 pptv in the free troposphere and 8 pptv in the marine boundary layer. Indeed, observations made by WFF and NOCAR were often at or below the stated detection limits, with some points appearing to lie outside of the stated precision (four values of NO measured by WFF lie below 0, although the stated detection limit and precision are 4 ± 4 pptv). However, the observed standard deviations, including ambient variability, for the 1-min averages are not shown here; the points do in fact fall within the stated values for detection limits and precision. Near 1400 (PDT) the aircraft encountered a plume of ship exhaust, but only 1 min of data was affected and removed from the data set. Evidence of significant layering in the free troposphere was observed in the NO_x, O_3, CO, and DPT data during the descent to the marine boundary layer. Sharp increases in the mixing ratios of the NO_x species and O_3 were encountered concurrent with a sharp decrease in DPT at about 1320 PDT during a spiral descent to the boundary

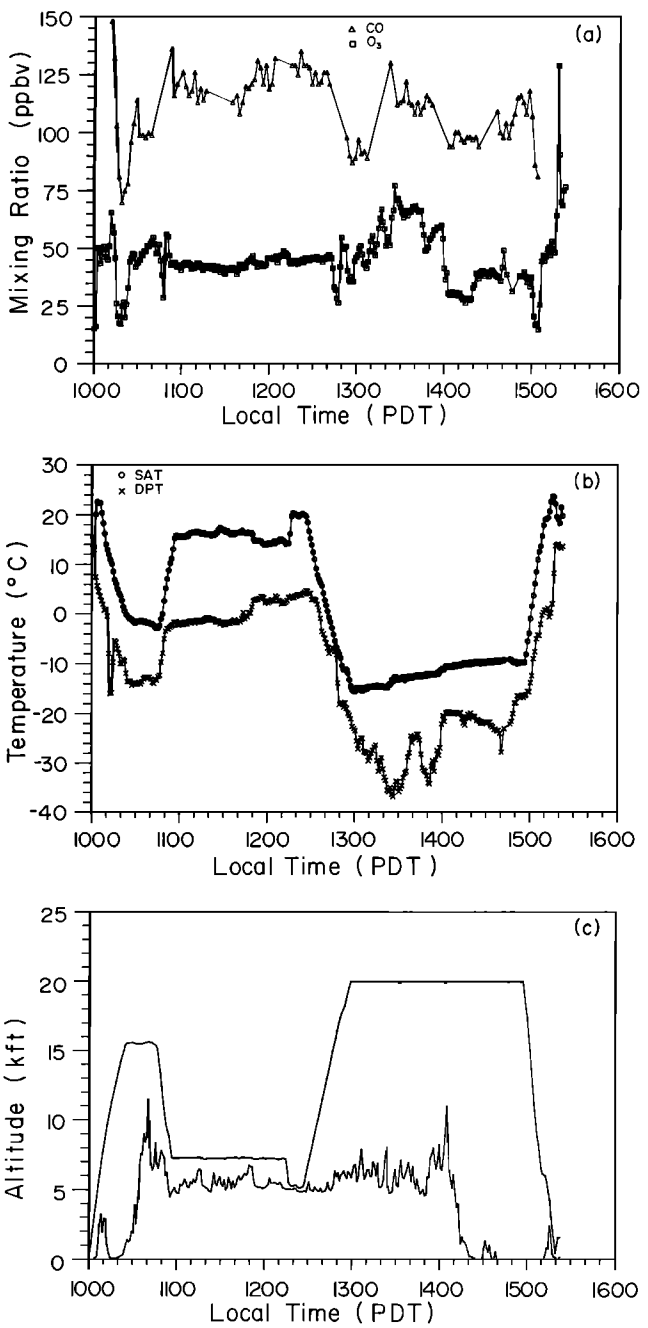

Fig. 10. September 2 trace species measurements: (*a*) O_3 and CO mixing ratios, (*b*) SAT and DPT, and (*c*) aircraft altitude and ground elevation.

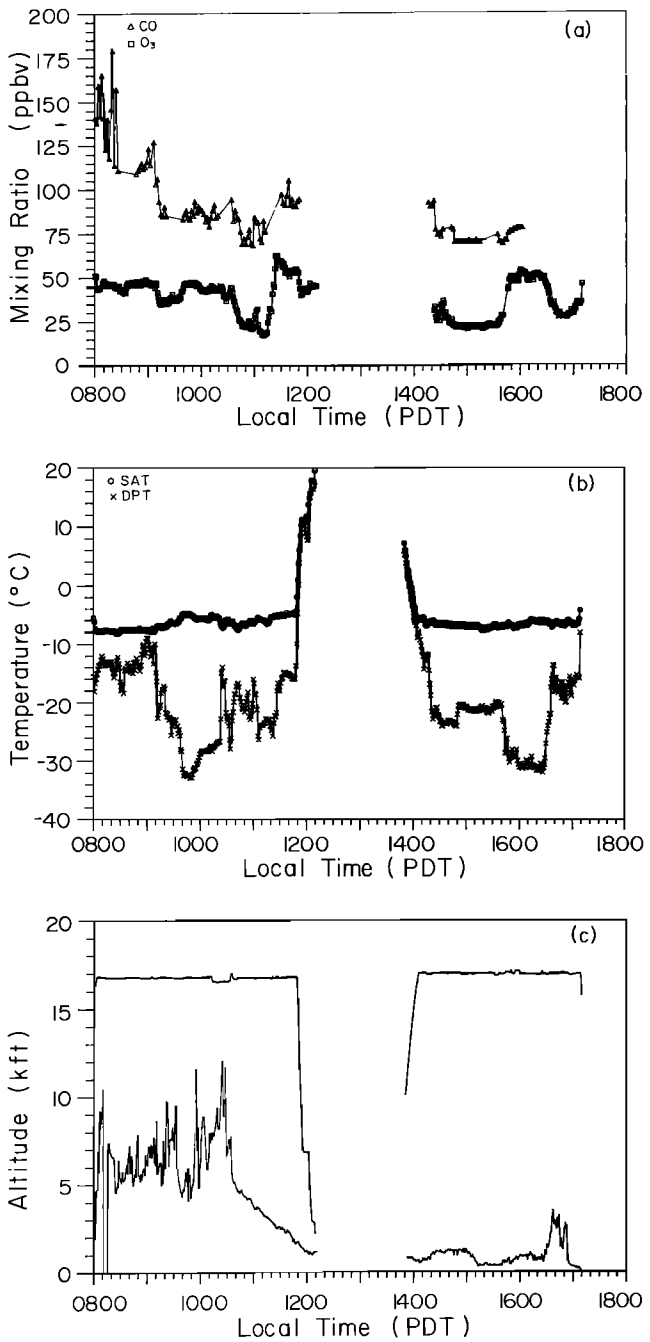

Fig. 11. September 5 trace species measurements: (*a*) O_3 and CO mixing ratios, (*b*) SAT and DPT, and (*c*) aircraft altitude and ground elevation.

layer. Similar evidence of atmospheric layering was also observed during other altitude profiles. In this case the anticorrelation among the mixing ratios of NO_x, O_3, and H_2O suggests that a layer of upper tropospheric air was entrained between layers of middle tropospheric air.

Flight 8 took place on August 21, 1986, and was conducted at 4.9 km with a single spiral descent to/ascent from ~ 0.3 km at the turnaround point near 1300 PDT. An mmct air mass was briefly encountered (1100-1115 and 1445-1500 PDT), but most of the observations were made in an mm air mass. The symmetry of the flight path is reflected in each of the species and temperature traces shown in Plates 4*a* and 4*b* and Figures 4*a*-4*c*. The lowest free tropospheric mixing ratios of NO, NO_2, and O_3 were seen to occur near the turnaround point with minima of about 20 pptv NO_x and 30 ppbv O_3. In both the NO and O_3 data, large variations were observed during the spiral descent/ ascent, again showing layering of the atmosphere that is often not represented by constant altitude measurements.

Flight 9 was a night flight conducted on August 23-24, 1986, over the western continental United States from Ames to northern Utah and southern Idaho. The flight was conducted at essentially constant altitude, with observations made at 4.6 km (15 kft) on the outbound leg and 4.9 km on the return leg. Mixing ratios of NO_2, O_3, and CO are presented in Plate 5 and Figure 5*a*, while traces of SAT and DPT are shown in Figure 5*b*, and aircraft altitude and ground elevation are shown in Figure 5*c*. Mixing ratios of NO were measured and reported by WFF only, and the average of 31 values was 0.7 ± 5 pptv, essentially zero, as expected for nighttime measurements. (Flights 1-3, carried out over the Atlantic, included periods of nighttime measurements, so that each group had the opportunity to ascertain that their instruments were performing properly.)

Maritime air and lower species mixing ratios were encountered initially near the coast; as the outbound leg reached further east, the air mass changed to mixed marine and continental, and reduced O_3 and NO_2 were observed from 2300 to 2400 PDT associated with leaving a region of nocturnal convection. *Shipham et al.* [this issue] show that the planetary boundary layer was deep, often extending to heights above that of the aircraft altitude. This is reflected in the traces of O_3 and DPT, and especially in the observed variability and elevated mixing ratios of NO_2 (2220-2320 and 0000-0055 (PDT)).

Flight 10 was conducted on August 26, 1986, and consisted of multilevel flight legs (Figure 6*c*) over the Pacific Ocean. Significant changes are again observed in mixing ratios and DPT with the transition from the free troposphere to the marine boundary layer as are shown in Plates 6*a* and 6*b* and Figures 6*a* and 6*b*. Mixing ratios of NO_2, O_3, and CO decreased significantly in the boundary layer and lower free troposphere, by as much as a factor of 2-3; simultaneously, the observed variability decreased markedly for O_3 and CO, although the NO data show an increase in both abundance and variability. In this instance the transition from free troposphere to boundary layer occurs following a transition from mt to mp air, compounding interpretation. The air mass was categorized as mm as the trajectory analysis showed a split flow of mt air from the south-southwest and mp air from the west-southwest [*Shipham et al.*, this issue].

Flight 11 was conducted on August 28, 1986, and consisted of multialtitude flight legs over the San Joaquin-Sacramento valleys of interior California. NO_x observations were made at ~2.5 km (7.5-8.5 kft), ~4.7 km (15.5 kft), and 3.8 km (12.5 kft) and are shown along with CO

TABLE 1. Model Runs

Flt	Run	ALT	T	DPT	CO	O_3	NO	NO_2	$P(O_3)$	C_2H_6	C_3H_8	C_2H_4	C_3H_6	Air Mass	Local Time
4	1	4.9	-5	-7	90	64	13	22	-1.0e6	700	250	100	40	mt	0925-0930
4	2	4.9	-5	-6	90	64	25	55	-2.0e5	700	250	100	40	mt	0930-0940
4	3	4.9	-5	-5	90	64	29	61	+2.3e5	700	250	100	40	mt	0940-0950
4	4	4.9	-5	-32	90	46	25	15	+5.2e5	550	100	50	20	mc	1050-1100
4	5	4.9	-5	-29	90	29	14	10	+2.4e5	550	100	50	20	mc	1100-1105
5	1	4.9	-3	-28	90	54	13	22	-4.2e4	900	60	20	20	mtcp	1430-1500
5	2	4.9	-2	-4	140	52	19	31	-6.6e5	1250	140	100	25	mc	1525-1550
5	3	4.9	-2	-7	125	70	19	46	-8.4e5	1250	220	125	40	mc, mpct	1645-1740
6	1	4.9	-5	-11	80	72	22	28	-9.4e5	1000	40	20	50	mt	1209, 1218
6	2	4.9	-5	-15	75	74	24	21	-8.1e5	1100	80	80	30	mt	1228, 1244
6	3	4.9	-5	-30	80	100	25	50	+5.4e4	1100	90	110	30	mt	1253
6	4	4.9	-5	-18	80	48	13	17	-2.1e5	750	20	40	20	mp, mt	1302, 1340, 1349 1359, 1410, 1928
6	5	4.9	-5	-11	75	68	29	39	-5.3e5	850	30	20	20	mt	1506, 1515
6	6	4.9	-5	-11	75	68	26	42	-4.8e5	850	30	20	20	mt	1524, 1535
7	1	4.9	-4	-22	57	24	4	11	-1.6e5	420	20	20	20	mt	1120-1145
7	2	4.9	-4	-18	57	24	9	6	-5.4e4	420	20	20	20	mt	1211-1229
7	3	0.2	+16	+13	65	30	.001	8	-2.5e6	900	50	65	40	mt	1326-1355
8	1	4.9	-4	-23	90	48	11	14	-1.5e5	760	46	68	20	mm	1117-1152
8	2	4.9	-3	-23	90	52	8	14	-4.8e5	760	60	68	20	mm	1352-1410
10	1	4.9	-4	-27	105	62	15	29	-3.3e4	900	75	65	20	mt	1128-1136
10	2	4.9	-4	-12	105	52	8	23	-6.4e5	900	75	65	20	mp	1140-1149
10	3	0.2	+16	+15	80	18	12	16	+1.6e5	750	30	150	100	mp	1246-1321
10	3*								-3.8e5						
11	1	2.6	+11	-1	72	35	10	20	-6.0e5	650	20	35	30	mmct	1141-1145
11	2	2.6	+11	-1	88	55	12	33	-1.4e6	650	20	35	30	mmct	1150-1154
11	3	4.7	-3	-29	120	64	10	20	-2.1e5	1050	70	75	20	mm	1245-1311
11	4	3.8	+3	-4	68	26	5	15	-6.1e5	525	20	20	20	mmct	1358-1424
12	1	5.0	-6	-17	85	46	12	15	-2.2e5	760	35	55	20	mm	1115-1119
12	2	5.0	-6	-17	85	40	12	9	-1.6e5	760	35	55	20	mm	1127-1201
12	6	1.0	+12	+5	85	18	2	5	-1.4e6	1160	25	130	55	mm	1250-1305
12	3	2.3	+12	-1	85	34	8	12	-1.3e6	880	45	125	50	mm	1322-1339
12	4	2.3	+14	-31	105	58	18	19	+2.8e5	880	45	50	20	mp	1344-1348
12	5	2.3	+14	-31	105	50	15	30	+2.1e5	880	45	50	20	mp	1352-1400
13	1	4.7	-3	-30	115	66	24	31	+3.6e5	800	60	95	20	mp	1115-1124
13	2	4.7	-3	-22	90	52	14	16	-4.3e4	700	40	65	20	mpct, mp	1133-1159
13	3	4.7	-3	-10	90	46	16	29	-3.1e5	1060	90	80	30	mpct	1252-1301
13	4	4.7	-5	-22	90	60	17	38	+2.1e4	1060	90	80	30	mpct	1315-1333
13	5	5.0	-7	-15	100	50	20	35	+1.6e5	1060	90	80	30	mpct	1342-1400
13	6	5.0	-7	-28	125	58	22	28	+3.8e5	500	225	170	25	mp	1444-1453
13	7	5.0	-7	-10	125	54	28	62	+4.9e5	500	225	120	25	mp, mpct	1436, 1502, 1511
13	8	5.0	-7	-22	125	75	15	25	-1.7e5	500	225	170	25	mpct	1520-1529
14	1	4.7	-2	-13	100	50	8	17	-5.6e5	550	25	60	20	mp	1038-1046
14	2	2.1	+15	0	125	42	40	60	+2.2e6	840	80	100	20	mpct	1131-1148
14	3	2.1	+15	0	125	42	69	131	+5.3e6	840	90	100	20	mpct	1157-1215, 1234
14	4	6.1	-10	-35	90	40	10	10	+3.4e4	700	6	50	20	mp	1301-1309
14	5	6.1	-10	-35	110	70	17	23	+6.2e4	1000	115	90	20	mp	1318-1327
14	6	6.1	-10	-22	110	38	9	11	-2.0e5	640	35	60	20	mp	1430-1448
15	1	5.2	-8	-13	115	46	21	35	+2.9e5	820	90	95	20	mpct/mc	0830-0907
15	2	5.2	-6	-23	90	38	11	17	+7.2e4	620	25	55	25	mp	0916-0934
15	3	5.2	-6	-32	90	46	15	23	+1.6e5	620	25	55	25	mp	0943-1040
15	4	5.2	-7	-20	75	24	7	3	-3.2e4	500	25	25	20	mp/mpct	1049-1115
15	5	5.2	-5	-15	95	55	20	24	-2.8e5	880	25	25	20	mpct/mc	1124-1151

TABLE 1. (continued)

Flt	Run	ALT	T	DPT	CO	O_3	NO	NO_2	$P(O_3)$	C_2H_6	C_3H_8	C_2H_4	C_3H_6	Air Mass	Local Time
16	1	5.2	-7	-24	75	26	10	14	+1.3e5	650	25	30	60	mc	1432-1441
16	2	5.2	-7	-22	75	21	6	12	+3.6e4	700	30	20	50	mc	1525-1534
16	3	5.2	-7	-31	75	50	11	29	+3.4e4	700	35	60	60	mc	1543-1609

Altitude in kilometers; T, DPT in degrees Celsius; CO, O_3 in parts per billion by volume; NO, NO_2, and hydrocarbons in parts per trillion by volume; $P(O_3)$, net ozone conversion rates, in molecules cm^{-3} s^{-1} (1.6e5 = 1.6 times 10^5); local time EDT for flights 4 and 5, and PDT for flights 6-16; mt, maritime tropical; mm, mixed maritime; mp, maritime polar; mc, mixed continental; mtcp, maritime tropical mixed with continental polar; mpct, maritime polar mixed with continental tropical; mmct, mixed maritime mixed with continental tropical.

*Same case without hydrocarbons.

and O_3 mixing ratios, SAT and DPT traces, and altitude and ground elevation in Plates 7*a* and 7*b* and Figures 7*a*-7*c*. Two air masses were encountered, mm (with a tendency for mp air aloft and mt air at lower levels) and mmct. The differences in the origin of the flow are reflected in the dew-point temperatures and the mixing ratios of all of the species. Initially, NO_x measurements were obtained in clean, mt air, as reflected by the species mixing ratios. Near 1150 (PDT) a deepening of the planetary boundary layer was encountered with enhanced values of the species and greater variability in the DPT and O_3 data. From 1240 until 1330 (PDT), measurements were made in the free troposphere in mm (dominated by mp) air with a minimum in DPT (1240-1300) and maxima in CO and O_3. Atypically, we do not see corresponding maxima in the NO_x data at this time. However, data obtained in the continental boundary layer are often similar to or greater than those obtained in the free troposphere, and in both of these environments the mixing ratios are enhanced relative to those obtained, for example, near 1130 (PDT).

Flight 12 was conducted on August 30, 1986, and consisted of multialtitude flight levels over the Pacific Ocean. Maritime polar air was encountered at 1100-1115 and 1345-1500 PDT, and mm air was encountered from 1115-1345 PDT. Observations at 5.0 km (16.5 kft) showed fairly uniform mixing ratios of NO around 12 pptv and decreasing values of NO_2 (Plates 8*a* and 8*b*). The 5.0-km leg was followed by a spiral descent to and a brief period of measurements at 1.0 km (3.3 kft), ascent to 2.3 km (7.5 kft) for period of 1 hour, a second briefperiod at 1.0 km, and an ascent to 4.7 km (see Figure 8*c*). A clear gradient with altitude is seen in Plates 8*a* and 8*b* and Figures 8*a* and 8*b* for all species but CO, with the lowest NO and O_3 mixing ratios observed during the 1.0-km-altitude legs. Additionally, although the aircraft was at constant altitude at 2.3 km from about 1305 to 1405 PDT, a significant increase in NO, NO_2, and O_3, along with a sharp decrease in DPT, was observed during the transition from mm (dominated by mt) to mp air masses beginning just after 1330 PDT. Although the enhanced species' mixing ratios suggest some degree of continental influence, this is not supported by the available meteorological data [*Shipham et al.*, this issue].

Flight 13, conducted on August 31, 1986, consisted of an outbound leg at 4.7 km over California, Nevada, and Arizona with a return leg at 5.0 km. Mixing ratios of NO, NO_2, CO, and O_3 are presented in Plates 9*a* and 9*b* and Figure 9*a*; SAT, DPT, altitude, and ground elevation are shown in Figures 9*b* and 9*c*. Maritime polar air was encountered at 1110-1130, 1145-1215, and 1440-1500 PDT, while mpct air was encountered during the remaining periods, 1130-1145, 1215-1440, and 1500-1530 PDT. Considerable variability in seen in the DPT traces and in the mixing ratios, associated with changes in air mass and indicative of air below the continental boundary layer. Indeed, *Shipham et al.* [this issue] state that the aircraft flew near the top of the planetary boundary layer during much of this flight.

Flight 14 was carried out on September 2, 1986, and consisted of flight legs at 4.9 km, 2.2 km (7.3 kft), 1.7 km (5.5 kft) and 6.1 km (20 kft) over California and Nevada to the Utah border (Figure 10e). The beginning and ending periods of observation were within mp air (1025-1045 and 1257-1455 PDT, at 4.7 km and 6.1 km, respectively), while maritime air mixed with ct air was encountered during the remainder of the flight (1055-1212 at 2.2 km and 1217-1225 at 1.6 km). Again, significant changes are observed with the transition from 4.7 km to 2.2 km and again from the boundary layer measurements at 1.6 km to the free troposphere at 6.1 km. In this instance the highest values obtained in the boundary layer correspond to ground-based sources of exhaust. Indeed, most values of NO_x are <50 pptv in the free troposphere over the continent, in contrast to values of 130-220 pptv in the continental boundary layer. However, low mixing ratios such as those encountered in the free troposphere during this flight were not atypical for an air mass with a maritime origin.

Flight set 15-16, conducted on September 5, 1986, consisted of the return from Moffett Field, California, to

Wallops Island, Virginia, with a stop at Tinker Air Force Base in Oklahoma. The flights were carried out at constant altitude as shown in Figure 11*c*. Mixing ratios of NO, NO_2, O_3, and CO are shown along with SAT and DPT traces in Plates 11*a* and 11*b* and Figures 11*a* and 11*b*. Several air masses were encountered on this set of flights, resulting in considerable variability in the mixing ratios of each of the species, and particularly in dew-point temperature. The air mass categories encountered were mp (0800-0840 and 0910-1100 PDT), mpct (0840-0900 and 1100-1130 PDT), and mc (0900-0910, 1130-1150, and 1410-1700 PDT). Mixing ratios of NO near the end of the flight were near zero, as the local time was near 2000 EDT and the sun was setting. The lowest values of NO_x and O_3 were encountered at about 1440-1540 in mc air masses with DPT of -21 C. Values changed abruptly at about 1550 when DPT dropped sharply to -30 C, O_3 increased from 25 ppbv to 50 ppbv, and NO_2 increased from ~10 pptv to ~30 pptv.

DISCUSSION

Air Mass Categories and NO_x Data Sets

In addition to the average NO_x data set described earlier (a set of 1-min average NO_x values generated from the average NO and average NO_2 data sets presented in Plates 1-11, designated ave NO_x), a second NO_x data set was generated from the observations of NO and NO_2 and analyzed according to air mass type for comparison: a set of all NO_x values determined from all the NO and NO_2 data submitted, regardless of integration time (midpoint times of the period of averaging were used), designated all NO_x. In this case, all of the values submitted by York (including NO_2 <50 pptv), GIT, WFF (NO only), and NOCAR were included in two data files: all NO and all NO_2. Simultaneous NO and NO_2 values were then summed to create the all NO_x data set. The results of the correlation analyses using the ave NO_x and all NO_x data sets are almost identical. The value, then, of using the set which employs all of the NO_x mixing ratios, all NO_x, is that it does not mathematically bias the NO_x values in any direction and there is 29% more data in the all NO_x data set (N = 1637) than in the ave NO_x data set (N = 1280). The results of the correlation analyses that employ the all NO_x data set follow. The time base used was that of the NO_x data set unless the other parameter had fewer data points, as was true for CO in all but two air mass categories, in which case the CO time base was employed. In each case, selecting the time base of the species with the smaller number of data points enables the correlation analyses to most closely represent that that would result if only simultaneous measurements were used. It is important to note that using averaged or combined data sets (ave NO_x or all NO_x) does have a diluting effect on data analyses, as opposed to examining the data with respect to individual data sets submitted by WFF, York, GIT, or NOCAR. For example, the correlation between all NO_x (or ave NO_x) and O_3 is not nearly as crisp as that found between GIT NO_x (or NOCAR NO_x) and O_3.

A total of 49.1% of the NO and NO_2 data were obtained in maritime air masses, and 50.9% of the data were obtained in air masses determined to have a continental influence. Of the NO_x values determined from measurements of NO and NO_2 made in marine environments, we encountered mt air 13.1% of the time, mm air 40.7% of the time, and nearly half of the observations (46.2%) were made in mp air masses. Of the measurements made in maritime environments, 15.9% of the data were obtained in the boundary layer (0-1 km), 11.6 % at 1-3 km, and 72.5% in the middle free troposphere (3-6.5 km). For data collected in continental environments, 23.5% of the observations were made in mc air masses, 34.8% in mpct air, 39.3% in mmct air, and only 2.4% in mtcp air. No measurements of NO_x were made in the 0 to 1 km altitude range in continental environments; 19.7% and 83.8% of the data were obtained at 1-3 km and 3-6.5 km, respectively.

Maritime Data

Distribution plots of the NO and NO_2 obser-vations made in maritime environments, and calculated NO_x, are shown in Figure 12. The data have been divided into three altitude bins for analysis, 0-1 km, 1-3 km, and 3-6.5 km.

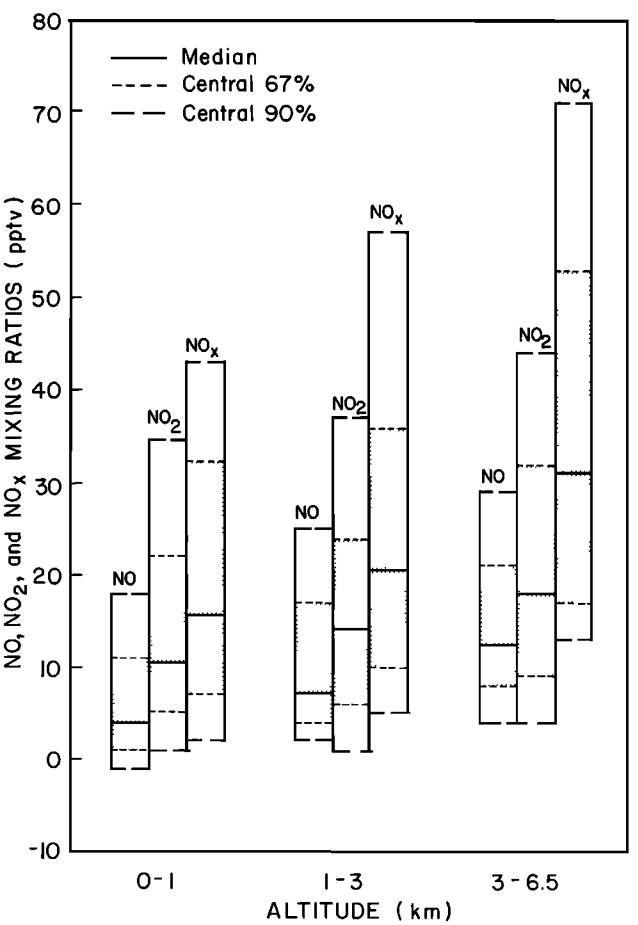

Fig. 12. Median values of NO, NO_2, and NO_x as determined from measurements of NO and NO_2 made in maritime air masses.

TABLE 2. Maritime Mean Values Plus or Minus Standard Deviations

NO_x (pptv)	O_3 (ppbv)	CO (ppbv)	DPT (C)	Restrictions
32.0 ± 25.6 (803)	42.4 ± 16.4 (803)	89.3 ± 19.9 (534)	-12.7 ±13.8 (803)	Maritime air masses*
25.1 ± 11.7 (678)	39.6 ± 15.0 (678)		-12.1 ± 14.2 (678)	$NO_x \leq 50$ pptv
20.3 ± 28.9 (128)	23.2 ± 6.9 (128)	84.9 ± 7.5 (75)	+11.7 ± 3.8 (128)	0-1 km
18.5 ± 12.5 (124)				$NO_x < 100$ pptv
24.1 ± 16.1 (93)	34.5 ± 12.9 (93)	86.5 ± 18.3 (60)	-3.2 ± 9.8 (93)	1-3 km
35.9 ± 25.1 (582)	47.9 ± 14.6 (582)	90.5 ± 21.6 (399)	-19.6 ± 7.1 (582)	3-6.5 km
34.3 ± 17.8 (575)				$NO_x \leq 100$ pptv
30.1 ± 36.5 (105)	34.9 ± 13.8 (105)	59.9 ± 3.1 (30)	-4.3 ± 13.7 (105)	Air mass category mt
27.4 ± 23.9 (104)				$NO_x \leq 100$ pptv
19.9 ± 11.9 (92)	31.2 ± 9.8 (92)			$NO_x \leq 50$ pptv
26.3 ± 50.2 (37)	30.8 ± 1.9 (37)	(0)	+12.4 ± 3.1 (37)	0-1 km
18.4 ± 14.5 (36)				$NO_x \leq 100$ pptv
33.1 ± 3.1 (9)	40.7 ± 4.9 (9)	(1)	-3.2 ± 2.5 (9)	1-3 km
32.1 ± 28.5 (59)	36.6 ± 17.8 (59)	59.6 ± 2.6 (29)	-14.9 ± 6.2 (59)	3-6.5 km
			-18.8 ± 2.4	-40 ≤ DPT ≤ -10
			-6.2 ± 0.8	-10 ≤ DPT ≤ +20
25.8 ± 26.2 (327)	36.8 ± 15.8 (327)	89.7 ± 13.8 (327)	-7.6 ± 14.8 (327)	Air mass category mm
22.4 ± 11.1 (308)				$NO_x \leq 50$ pptv
18.7 ± 12.4 (81)	19.2 ± 2.9 (81)	85.9 ± 5.9 (81)	+12.0 ± 3.8 (81)	0-1 km
20.1 ± 13.5 (60)	30.1 ± 10.8 (60)	84.6 ± 12.6 (60)	+0.3 ± 6.5 (60)	1-3 km
30.7 ± 32.1 (186)	46.7 ± 12.3 (186)	92.9 ± 15.7 (186)	-18.8 ± 7.0 (186)	3-6.5 km
27.4 ± 13.6 (182)				$NO_x \leq 100$ pptv

TABLE 2. (continued)

NO_x (pptv)	O_3 (ppbv)	CO (ppbv)	DPT (C)	Restrictions
38.0 ± 19.2 (371)	49.5 ± 14.6 (371)	96.0 ± 21.3 (252)	-19.6 ± 8.8 (371)	Air mass category mp
36.6 ± 16.0 (361)				$NO_x \leq 75$ pptv
29.7 ± 10.7 (278)	45.9 ± 13.2 (278)			$NO_x \leq 50$ pptv
11.3 ± 6.8 (10)	27.5 ± 11.1 (10)	94.0 ± 3.5 (5)	+6.4 ± 2.1 (10)	0-1 km
30.8 ± 21.6 (24)	43.2 ± 14.6 (24)	101.5 ± 21.1 (17)	-11.8 ± 12.9 (24)	1-3 km
39.3 ± 18.7 (337)	50.6 ± 14.1 (337)	95.7 ± 21.6 (230)	-20.9 ± 6.9 (337)	3-6.5 km
38.5 ± 16.2 (334)				$NO_x \leq 100$ pptv

Numbers in parentheses are total number of data points included in each average.
*All maritime data; mt, maritime tropical; mm, mixed maritime; mp, maritime polar.

A positive gradient with altitude was observed for the NO_x species. The median value of NO_x in the marine boundary layer was 15.7 pptv, while that for the middle free troposphere (3-6.5 km) was 31.0 pptv. Whereas median values are given here in the text, averages plus or minus the standard deviations (including instrument and atmospheric variability) of the mixing ratios of NO_x, O_3, and CO observed in maritime air masses are shown in Table 2 along with dew-point temperature measurements. The data have been divided according to air mass category and altitude, and the total number of data points included in each average is given in parentheses. In several cases, additional values are listed using a filter for NO_x of ≤100 pptv and/or ≤50 pptv so that the data may be presented in the most representative manner. For example, the average value of NO_x in boundary layer (0-1 km) maritime tropical air (category mt) is 18.4 ± 14.5 pptv when one outlier value ($NO_x \geq 100$ pptv) is ignored. In the maritime data set, these outliers typically correspond to spikes where pollution was encountered (e.g., aircraft exhaust in flight 6), and represent values that are factors of 2-3 times higher than neighboring points. O_3 is typically well correlated with NO_x in the maritime data set; thus the positive gradient with altitude observed for O_3 (Table 2) is expected. In the marine boundary layer, O_3 averaged 23.2 ± 6.9 ppbv, while the mean O_3 mixing ratio in the middle free troposphere in maritime air masses was 47.9 ± 14.6 ppbv. Dew-point temperature, as expected, also shows a gradient with altitude, with typical marine boundary layer values of +12 C and typical free tropospheric values of ~-20 C. In contrast, CO values did not vary significantly with altitude. However, lower values of CO (60 ppbv) were observed in mt air than were observed in mm and mp air masses, where CO mixing ratios were typically 85-100 ppbv. Perhaps the mt air masses encountered during this period were more highly aged than were the mp and mm air masses.

Correlation coefficients for NO_x with O_3, DPT, and CO are given in Table 3, and correlation coefficients for O_3 with DPT and CO, and CO with DPT, are listed in Table 4. Again the data have been divided according to air mass category and altitude, and filters for NO_x are included to show the degree of correlation most representative of the data sets. The total number of data points included in each analysis is given in parentheses, and correlation coefficients that are not significant at the 95% confidence level are indicated by a dagger. The level of significance determined in these analyses assumes that the number of degrees of freedom equals the number of observations, and assumes that the extent of autocorrelation among the measurements is small, since the entire data set (including measurements made by different techniques for all of the flights) is used to derive the correlation relationships. Hence it is possible that the significance levels are artifically high due to autocorrelation among successive measurements, especially those made by similar techniques.

There is no evidence of significant correlation between NO_x and O_3 in the marine boundary layer; this is in line with previous data sets [e.g., *Ridley et al.*, 1987, 1988*a*, *b*, 1989] which show that the correlation between these species is rarely maintained for $O_3 \leq 30$ ppbv. As expected [*Ridley et al.*, 1987, 1988*a*, *b*, 1989], the degree of

TABLE 3. Maritime NO_x Correlations

$R(NO_x, O3)$	$R(NO_x, DPT)$	$R(NO_x, CO)$	Restrictions
+0.48 (803)	-0.22 (803)	+0.24 (534)	Maritime air masses*
+0.68 (773)	-0.37 (773)		$NO_x \leq 75$ pptv
+0.65 (678)	-0.42 (678)		$NO_x \leq 50$ pptv
+0.09 (128)†	+0.12 (128) †	+0.10 (75) †	0-1 km
+0.78 (93)	-0.74 (78)	-0.07 (60) †	1-3 km
+0.46 (582)	+0.06 (582)	+0.27 (399)	3-6.5 km
+0.63 (575)			$NO_x \leq 100$ pptv
+0.51 (105)	+0.10 (105) †	+0.59 (30)	Air mass category mt
+0.82 (104)	+0.002 (104) †		$NO_x \leq 100$ pptv
-0.04 (37) †	+0.02 (37) †		0-1 km
+0.83 (9)	-0.85 (9)		1-3 km
+0.89 (59)	+0.83 (59)	+0.50 (29)	3-6.5 km
	-0.28 (41) †		$-40 \leq DPT \leq -10$
	+0.79 (18)		$-10 \leq DPT \leq +20$
+0.35 (327)	-0.24 (327)	+0.19 (327)	Air mass category mm
+0.59 (308)	-0.39 (308)	+0.38 (308)	$NO_x \leq 50$ pptv
+0.02 (81) †	+0.27 (81)	+0.05 (81) †	0-1 km
+0.67 (60)	-0.73 (60)	-0.14 (60) †	1-3 km
+0.28 (186)	-0.08 (186) †	+0.18 (186)	3-6.5 km
+0.53 (182)	-0.13 (182) †		$NO_x \leq 100$ pptv
+0.55 (371)	-0.15 (371)	+0.18 (252)	Air mass category mp
+0.76 (10)	-0.27 (10) †	-0.62 (5) †	0-1 km
+0.85 (24)	-0.75 (24)	+0.32 (17) †	1-3 km
+0.49 (337)	+0.09 (337) †	+0.19 (230)	3-6.5 km
+0.60 (334)	+0.09 (334) †		$NO_x \leq 100$ pptv

Numbers in parentheses are total numbers of data points in each analysis.

*all maritime data; mt, maritime tropical; mm, mixed maritime; mp, maritime polar.

† Correlation coefficients are not significant at the 95% confidence level.

correlation between NO_x and O_3 is high in the lower and middle free troposphere, particularly so when only NO_x values ≤100 pptv are included in the analysis. Approximately 98% of the data are included in such a filter; indeed, 84.4% of the NO_x values are ≤50 pptv in the maritime data set.

Similarly, there is a lack of significant correlation between NO_x and DPT in the marine boundary layer in all but mm air, where a weak negative correlation is observed. The highest degree of correlation observed for these species routinely occurs in data obtained at 1-3 km in each maritime air mass category. In this data subset, NO_x and DPT are strongly anticorrelated. Generally, with DPTs high in the boundary layer and lower in the free troposphere and with the opposite gradient for NO_x one might expect to observe a negative correlation between NO_x and DPT throughout the troposphere. Interestingly, the correlation observed at 1-3 km typically disappears in the upper free troposphere. Indeed, only in mt air is there a strong correlation between NO_x and DPT measurements made at 3-6.5 km, and the correlation is positive. In this case the correlation in governed by the 18 points falling in the regime where DPT is unusually high for the middle free troposphere (-10 to +20 C). Stratospheric input to the troposphere would likely result in a high degree of anticorrelation between NO_x and DPT, bringing air masses rich in NO_x but low in water vapor. Thus observations of no significant or positive correlation between NO_x and DPT in the middle free troposphere argue against stratospheric input. Conversely, lightning occurring in the upper free troposphere might represent an option for increased NO_x mixing ratios in regions of higher water vapor, which

TABLE 4. Maritime Supporting Measurements Correlations

$R(O_3, DPT)$	$R(CO, DPT)$	$R(O_3, CO)$	Restrictions
-0.62 (803)	-0.22 (534)	+0.37 (534)	Maritime air masses*
-0.29 (128)	+0.19 (75) †	+0.08 (75) †	0-1 km
-0.84 (93)	-0.19 (60) †	+0.30 (60)	1-3 km
-0.20 (582)	-0.28 (399)	+0.39 (399)	3-6.5 km
	+0.57 (336)	$NO_x \leq 50$ pptv	
+0.10 (105) †	+0.77 (30)	+0.73 (30)	Air mass category mt
-0.86 (37)		0-1 km	
-0.46 (9) †		1-3 km	
+0.91 (59)	+0.68 (29)	+0.66 (29)	3-6.5 km
-0.89 (327)	-0.45 (327)	+0.60 (327)	Air mass category mm
-0.63 (81)	+0.45 (81)	-0.05 (81) †	0-1 km
-0.92 (60)	-0.18 (60) †	+0.25 (60) †	1-3 km
-0.73 (186)	-0.71 (186)	+0.77 (186)	3-6.5 km
-0.25 (371)	-0.04 (252) †	+0.10 (252) †	Air mass category mp
-0.21 (10) †	+0.57 (5) †	-0.48 (5) †	0-1 km
-0.75 (24)	-0.09 (17) †	+0.48 (17) †	1-3 km
-0.04 (337) †	-0.07 (230) †	+0.09 (230) †	3-6.5 km

Numbers in parentheses are total number of data points included in each analysis.
*all maritime data; mt, maritime tropical; mm, mixed maritime; mp, maritime polar.
† Correlation coefficients are not significant at the 95% confidence level.

might explain the positive correlation observed for the 18 points mentioned above. However, it is also possible that the air outside electrically active clouds would be low in water vapor; in that case a negative correlation would be expected.

NO_x and CO are typically only weakly positively correlated in the middle free troposphere. The degree of correlation between NO_x and CO increases for data obtained in mm air when only all NO_x values of ≤50 pptv are considered. However, it is difficult to draw conclusions from this data set because of the sparsity of the CO data in the marine boundary layer and lower free troposphere, especially in mt and mp air masses.

After examining the correlations among NO_x, O_3, and DPT, we expect and typically find a high degree of anticorrelation between O_3 and DPT. If the O_3 in the troposphere has its origin in the stratosphere, a strong negative correlation is expected between O_3 and DPT at the highest altitudes. The behavior of these species in mm air masses is consistent with such a source. However, a strong positive correlation is observed between O_3 and DPT in mt air masses at 3-6.5 km, and no significant correlation is observed between these species in mp air masses at 3-6.5 km. Given the previous discussion of the correlations among NO_x, O_3, and DPT, the lack of correlation at 3-6.5 km in mp air masses is expected. As mentioned above, the period of atypically high DPT in mt air masses at 3-6.5 km dominates the correlations between DPT and the other species to the extent that the signs of the correlations are opposite to those observed in the other air mass categories. Tropical storm activity could mix updrafted marine boundary layer air containing higher mixing ratios of water vapor with the higher mixing ratios of O_3 typically found in upper free tropospheric air.

Although no significant correlation is observed between O_3 and CO in mp air masses, a positive correlation is observed between these species in mm and mt air masses at 3-6.5 km. The correlation between CO and DPT flips between positive and negative, within a single air mass category (mm) and in the 3 to 6.5-km-altitude data (positive in mt air and negative in mm air). Again, there is little CO data in the marine boundary layer and lower free troposphere in two of the three air mass categories, so that conclusions that contrast the various categories are difficult to draw. However, both stratospheric influence and boundary layer updrafts might be evidenced by positive correlations between CO and DPT, depending on the age of the air mass in the case of boundary layer air.

As noted above, the greatest number of observations were made at 3-6.5 km (72.5%), and 57.9% of these were made in mp air masses, 32.0% in mm air masses, and only 10.1 % in mt air masses. In comparing mean NO_x values in the different maritime categories, no significant differences are observed, given the standard deviations listed in Table 2. Nonetheless, both the lowest (11.3 ± 6.8 pptv) and highest (38.5 ± 16.2 pptv) mean values of NO_x were

encountered in mp air, in the boundary layer and middle free troposphere, respectively. Of the data obtained at 1-3 km, 64.5% fall into the mm air mass category, and their mean value of NO_x (20.1 ± 13.5 pptv) is lower than that of the other two categories (mt, 33.1 ± 3.1; mp, 30.8 ± 21.6 pptv). The lowest values of O_3 in the marine boundary layer and lower free troposphere were encountered in mm air masses, while the lowest middle free tropospheric mean O_3 value falls into the mt category. As previously mentioned, the lowest CO values were encountered in mt air, and the highest mean CO values were found in mp air masses. However, it must be noted that only 5.6% of the CO data fall into the mt category, while 47.2% of the CO data were obtained in mp air masses. As expected, mp air was drier than mt air, as reflected in the dew point temperatures listed in Table 2. In summary, then, with exceptions as noted above, higher values of NO_x, O_3, and CO were typically encountered in the drier mp air.

Continental Data

Distribution plots of the NO and NO_2 observations made in continental environments, and calculated NO_x, are shown in Figure 13. In this case the data have been divided into two altitude bins for analysis, 1-3 and 3-6.5 km (height above sea level). A negative gradient with increasing altitude was observed for the NO_x species in continental environments. The median value of NO_x at 1-3 km was 118.3 pptv, while that at 3-6.5 km was 51.0 pptv. It is difficult to separate boundary layer data from free tropospheric data in the continental environments in this data set because boundary layer heights sometimes exceeded Electra flight altitudes. Still, the influence of the continent with fresh sources of pollution is clearly seen in the data obtained at 1-3 km. Mean values plus or minus the standard deviations (including instrument and atmospheric variability) of the mixing ratios of NO_x, O_3, and CO and DPT observed in continental air masses are shown in Table 5. The data have again been divided according to air mass category and altitude, and the total number of data points included in each average is given in parentheses. In several cases, additional values are listed using a filter for NO_x of ≤150, 100, 75 and/or 50 pptv so that the data may be presented in the most representative manner (in the case of a few outlier points) or to show that the mixing ratios were generally higher in the continental data set, as seen by using the same filters as those discussed in the maritime data. For example, in the mpct air mass category, ~30 % of the NO_x values are >100 pptv. There is a slight positive gradient when the highest NO_x values (typically associated with the freshest sources of pollution) are discarded, and the correlation between O_3 and NO_x in the continental data set is much improved. In the continental data, O_3 averaged 37-43 ppbv at 1-3 km, while the mean O_3 mixing ratio at 3-6.5 km was 49-52 ppbv. Dew-point temperature variations were similar to those previously discussed for the maritime data set, although the driest air of the entire data set was encountered (on the

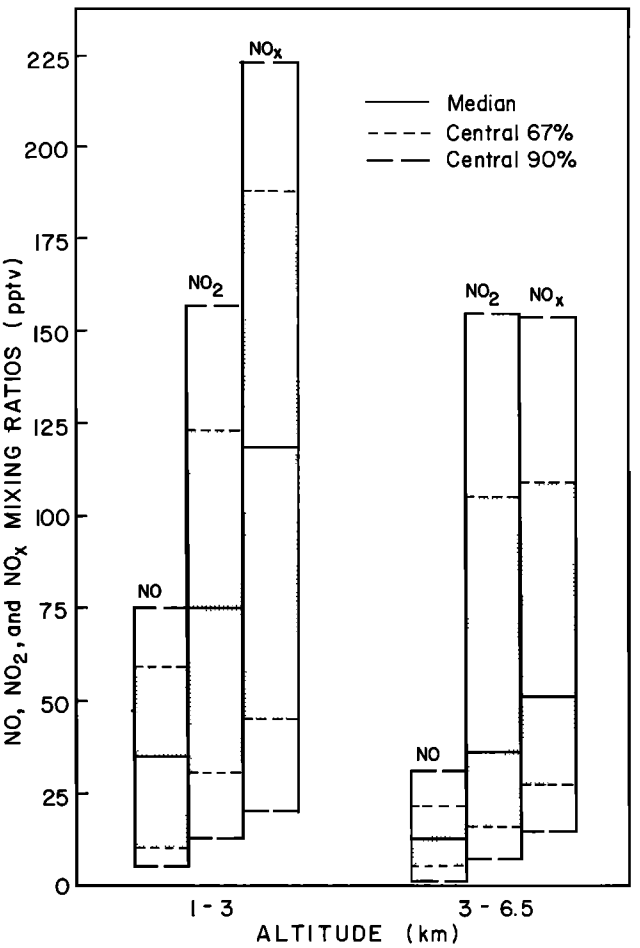

Fig. 13. Median values of NO, NO_2, and NO_x as determined from measurements of NO and NO_2 made in continental air masses.

average) in the rather sparse subset of mtcp air masses (-27 C). CO values did not vary in any routine fashion. In mmct air masses, CO values at 1-3 km were significantly smaller than those found at 3-6.5 km, whereas the reverse was true for CO values obtained in mpct air masses. Again, this may suggest a stratospheric influence in the mp air masses resulting in lower mixing ratios of CO at 3-6.5 km. Additionally, mean CO values obtained at 3-6.5 km in mc and mtcp air masses were somewhat lower than mean CO values obtained in the other continental air mass categories. The somewhat uncertain division of the data into mixed air mass categories would likely cloud strong signatures for individual source regions.

Correlation coefficients for NO_x with O_3, DPT, and CO are given in Table 6, and correlation coefficients for O_3 with DPT and CO and CO with DPT are listed in Table 7. Once again, the data have been divided according to air mass category and altitude, and filters for NO_x are included to show the degree of correlation most representative of the data sets. The total number of data points included in each analysis is given in parentheses, and correlation coefficients that are not significant at the 95% confidence level (assum-

TABLE 5. Continental Mean Values Plus or Minus Standard Deviations

NO_x (pptv)	O_3 (ppbv)	CO (ppbv)	DPT (C)	Restrictions
75.4 ± 56.0 (834)	47.3 ± 12.0 (834)	101.6 ± 23.6 (386)	-11.1 ± 9.1 (834)	Continental air masses*
47.9 ± 24.2 (613)				$NO_x \leq 100$ pptv
118.5 ± 68.2 (164)	42.1 ± 5.7 (164)	102.9 ± 26.2 (69)	-0.3 ± 3.4 (164)	1-3 km
65.0 ± 46.9 (699)	48.5 ± 12.7 (699)	99.9 ± 21.0 (304)	-13.8 ± 8.1 (669)	3-6.5 km
45.3 ± 48.1 (196)	45.0 ± 16.9 (196)	94.8 ± 22.9 (98)	-18.0 ± 9.5 (196)	Air mass category mc (all 3-6.5 km)
39.4 ± 22.2 (191)				$NO_x \leq 150$ pptv
35.2 ± 17.1 (176)				$NO_x \leq 75$ pptv
40.0 ± 9.2 (20)	52.1 ± 4.7 (20)	90.2 ± 5.5 (11)	-27.2 ± 2.8 (20)	Air mass category mtcp (all 3-6.5 km)
37.6 ± 5.1 (18)				$NO_x \leq 50$ pptv
91.1 ± 61.3 (290)	47.8 ± 9.5 (290)	108.3 ± 19.2 (133)	-8.4 ± 9.6 (290)	Air mass category mpct
54.1 ± 20.9 (194)				$NO_x \leq 100$ pptv
143.3 ± 55.6 (128)	43.4 ± 2.0 (128)	122.0 ± 6.32 (37)	+0.6 ± 2.5 (128)	1-3 km
49.9 ± 20.5 (162)	51.3 ± 11.5 (162)	103.1 ± 19.9 (96)	-15.5 ± 6.5 (162)	3-6.5 km
81.71 ± 49.0 (328)	47.9 ± 10.4 (328)	101.5 ± 19.0 (328)	-8.4 ± 9.6 (328)	Air mass category mmct
27.3 ± 20.9 (194)	37.7 ± 10.2			$NO_x \leq 50$ pptv
29.8 ± 13.4 (35)	37.4 ± 10.4 (35)	75.90 ± 9.9 (35)	-3.8 ± 3.9 (35)	1-3 km
88.4 ± 47.8 (291)	49.1 ± 9.7 (291)	104.5 ± 17.5 (291)	-9.15 ± 4.0 (291)	3-6.5 km

Numbers in parentheses are total number of data points included in each average.

*all continental data; mc, mixed continental; mtcp, maritime tropical mixed with continental polar; mpct, maritime polar mixed with continental tropical; mmct, mixed maritime mixed with continen- tal tropical.

TABLE 6. Continental NO_x Correlations

$R(NO_x, O3)$	$R(NO_x, DPT)$	$R(NO_x, CO)$	Restrictions
+0.29 (834)	+0.55 (834)	+0.52 (386)	Continental air masses*
+0.53 (613)	+0.37 (613)		$NO_x \leq 100$ pptv
		-0.17 (13)†	0-1 km
+0.50 (164)	+0.66 (164)	+0.75 (69)	1-3 km
+0.44 (669)	+0.45 (669)	+0.59 (304)	3-6.5 km
+0.52 (665)	+0.51 (665)		$NO_x \leq 200$ pptv
+0.25 (196)	+0.27 (196)	+0.81 (98)	Air mass category mc
+0.79 (176)	+0.43 (176)		$NO_x \leq 75$ pptv
+0.03 (20) †	+0.60 (20)	-0.16 (11) †	Air mass category mtcp (all 3-6.5 km)
-0.12 (290)	+0.76 (290)	+0.57 (133)	Air mass category mpct
+0.26 (194)	+0.58 (194)		$NO_x \leq 100$ pptv
+0.66 (128)	+0.72 (128)	+0.72 (37)	1-3 km
+0.58 (162)	+0.37 (162)	+0.49 (96)	3-6.5 km
+0.77 (328)	+0.17 (328)	+0.82 (328)	Air mass category mmct
+0.69 (110)	-0.48 (110)		$NO_x \leq 50$ pptv
+0.70 (35)	-0.60 (35)	+0.42 (35)	1-3 km
+0.77 (291)	+0.41 (291)	+0.80 (291)	3-6.5 km

Numbers in parentheses are total number of data points included in each analysis

*all continental data; mc, mixed continental; mtcp, maritime tropical mixed with continental polar; mpct, maritime polar mixed with continental tropical; mmct, mixed maritime mixed with continental tropical.

†Correlation coefficients are not significant at the 95% confidence level.

ing that the number of degrees of freedom equals the number of observations) are indicated by a dagger.

As mentioned above, the correlation between NO_x and O_3 in the continental data is significantly improved when the highest NO_x values are not included in the analyses. A high degree of correlation between NO_x and O_3 is not expected when sampling in environments near fresh sources of NO_x pollution, where balance between ozone production and destruction has not yet been achieved.

Whereas there tended to be a negative correlation between NO_x and DPT in the marine data set, a positive correlation is observed in all of the continental environ- ments except mmct air masses, where a negative correlation is observed for data obtained at 1-3 km only. In convective environments a positive correlation be- tween NO_x and DPT would be expected; moister air from below along with fresher sources of NO_x pollution is carried aloft. In many of the continental flights, measurements were made at midday, and the degree of convective activity was evidenced by boundary layer heights often surpassing flight altitudes of ~ 4.9 km. The mmct air masses at 1-3 km might have had their origin in the cleaner marine boundary layer where NO_x would be expected to be very low while DPT values would be high, thus resulting in a negative correlation between these species.

NO_x and CO typically have a much higher degree of correlation in data obtained in continental environments than was seen in the marine data . This is not surprising, since both NO_x and CO are emitted by pollution sources in the continental boundary layer. The exception is the very small subset of data collected in mtcp air masses. Again, if the origin of these air masses had a marine boundary layer influence, a strong correlation would not be expected. Similarly, the cp air masses may have experienced little pollution influence due to origins in less populated regions.

In three of the continental air mass categories, no correlation is observed between O_3 and CO in data obtained at 3-6.5 km. A positive correlation is observed between these species at 3-6.5 km only in the mc air mass category. Although the data sets at 1-3 km are considerably smaller, a positive correlation is observed between O_3 and CO in mpct air masses, and a negative correlation is observed for these species in mmct air

TABLE 7. Continental Supporting Measurements Correlations

$R(O_3, DPT)$	$R(CO, DPT)$	$R(O_3, CO)$	Restrictions
+0.08 (835)	+0.41 (386)	+0.52 (386)	Continental air masses*
	+0.72 (13)		0-1 km
-0.05 (164) †	+0.35 (69)	+0.58 (69)	1-3 km
+0.28 (669)	+0.43 (304)	+0.58 (304)	3-6.5 km
+0.57 (196)	+0.66 (98)	+0.73 (98)	Air mass category mc (all 3-6.5 km)
-0.38 (20) †	+0.02 (11) †	-0.01 (11) †	Air mass category mtcp (all 3-6.5 km)
-0.35 (290)	+0.60 (133)	+0.01 (133) †	Air mass category mpct
+0.67 (128)	+0.73 (37)	+0.39 (37)	1-3 km
-0.04 (162) †	+0.44 (96)	+0.19 (96) †	3-6.5 km
-0.24 (328)	-0.02 (328) †	+0.81 (328)	Air mass category mmct
-0.96 (35)	-0.76 (35)	+0.81 (35)	1-3 km
-0.02 (291) †	+0.25 (291)	+0.80 (291)	3-6.5 km

Numbers in parentheses are total number of data points included in each analysis.
*all continental data; mc, mixed continental; mtcp, maritime tropical mixed with continental polar; mpct, maritime polar mixed with continental tropical; mmct, mixed maritime mixed with continental tropical
† Correlation coefficients are not significant at the 95% confidence level.

masses. The correlation between CO and DPT is typically positive except in the case of data obtained at 1-3 km in mmct air masses. Finally, a strong positive correlation is observed between O_3 and CO in mc and mmct air masses. In contrast, no correlation is observed for these species in mtcp air masses or in data obtained at 3-6.5 km in mpct air masses.

Again, the greatest number of observations was made at 3-6.5 km (83.3%), and 43.5% of the data were obtained in mmct air masses, 29.3% in mc air masses, 24.2% in mpct air masses, and only 3.0 % in mtcp air masses. In comparing mean NO_x values in the different continental categories, significant differences are observed: NO_x mixing ratios observed in mc and mtcp air masses are considerably lower than those observed in mpct air masses and in data obtained at 3-6.5 km in mmct air. This would be expected if the primary source region of cp air were sparsely populated northwest Canada, while source regions of ct air masses likely include the populated California coastline and cities just inland. Indeed, the source regions of cp air masses predicted by the 60-hour back trajectories include northwest Canada. In contrast, however, while only 22% of the data obtained at 1-3 km fall into the mmct air mass category, the mean NO_x values are not very different from two of the maritime air mass categories and are considerably lower than values obtained in mpct air masses (78% of the 1 to 3 -km data). Perhaps, in this case, the mm air masses were dominant. The lowest values of O_3 and CO were also found at 1-3 km in mmct air. As previously mentioned, the highest values of CO values were encountered at 1-3 km in mpct air. As already noted, dew-point temperatures were lowest in mtcp air, and DPT values did not vary significantly among the other three air mass categories. In summary, then, the highest values of NO_x and CO were typically encountered at 1-3 km in mpct air.

Ozone Production/Destruction

Net ozone conversion rates, $P(O_3)$, were determined using a box model and the mechanism described by *Liu et al.* [1987]. $P(O_3)$ is the difference between the rates of formation and the rates of destruction of O_3. O_3 production rates include oxidation of NO by peroxy radicals such as HO_2, CH_3O_2, and higher RO_2, while O_3 destruction rates include photolysis to excited O atoms (O^1D) and their reaction with H_2O, and the reaction of O_3 with HO_2 and OH [cf. *Chameides et al.*, 1987; *Ridley et al.*, 1987, 1989]. CH_4 and its oxidation products as well as ethane, propane, ethylene, and propylene were considered in the model. $HO_2 + RO_2$ was included in the model in a generic fashion [*Trainer et al.*, 1987] (k = 3.0 times 10^{-12}], and $CH_3O_2 + CH_3O_2$ was also included, although the inclusion of the $RO_2 + RO_2$ chemistry is not anticipated to make a significant difference in calculated $P(O_3)$ [*Trainer et al.*, 1987]. $P(O_3)$ was determined from the model using as input ambient values of NO, O_3, CO, T, DPT, the hydro-

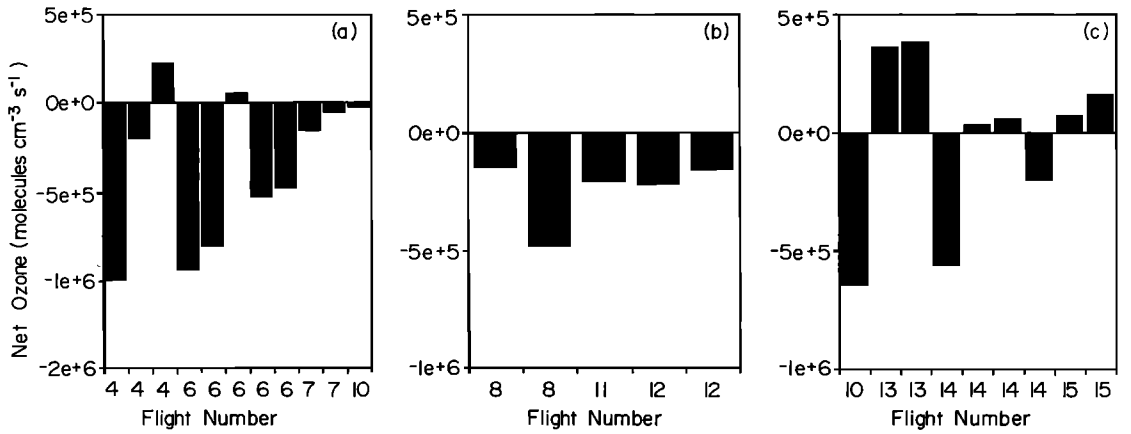

Fig. 14. Calculated net ozone conversion rates, $P(O_3)$, for the maritime middle free troposphere: (*a*) maritime tropical (mt) air masses, (*b*) mixed maritime (mm) air masses, and (*c*) maritime polar (mp) air masses.

carbons mentioned above, and J NO_2 values calculated from a second model that input the Eppley radiometer measurements of UV flux [*Madronich*, 1987]. (J NO_2 is the expression used to represent the rate constant for the photodissociation of NO_2: $NO_2 + h\nu \rightarrow NO + O(^3P)$.)

All photolysis rates were scaled according to the factor generated by comparing J NO_2 (model 2) with J NO_2 (model 1). The difference between these model-generated values was typically ≤10% for clear-sky conditions. A further discussion of the details of the box model and the results of model sensitivity studies is given by M. A. Carroll, et al., in a paper (in progress) that compares observed ratios of NO_2/NO with theoretically generated values and examines the NO_2/NO photostationary state with respect to calculated O_x (oxidant). Briefly, however, a 30% change in ambient ozone can result in a 50-150% change in $P(O_3)$ (depending on changes in the other parameters; although $P(O_3)$ is not well correlated with O_3, $P(O_3)$ tended to be negative for ambient O_3 >40 ppbv), and changes in dew-point temperature of 3 C can result in a 17-55% change in net ozone conversion rates. Generally, considering the uncertainty (including ambient variability) of the input parameters, values of $P(O_3) \geq \pm 1$ times 10^5 molecules cm^{-3} s^{-1} (0.02 ppbv $hour^{-1}$ at 5 km) may be considered as significantly different from 0.

As previously mentioned, the ambient values used in each model run and the net ozone conversion rates calculated are listed in Table 1 on a flight-by-flight basis. Ambient values of NO from the NOCAR data set only were used in the model runs, as that set had the most coverage and it is important to use an individual, rather than an average, data set to best observe differences in this type of analysis. Also, note that NO values were input, not NO_x. In this section, $P(O_3)$ will be discussed accord- ing to air mass category and altitude. $P(O_3)$ values calculated for data obtained at altitudes above 4.7 km are shown in the bar charts in Figures 14 and 15, while $P(O_3)$ values calculated for data obtained at altitudes below 4.7 km are shown in the bar chart in Figure 16. A bar chart is presented for each of the maritime air mass categories discussed above in Figure 14: (*a*) mt, (*b*) mm, and (*c*) mp. Similarly, three bar charts are presented for the continental air mass categories in Figure 15: (*a*) mc, (*b*) mpct, and (*c*) mixtures of the air mass categories.

As seen in the bar charts of Figures 14*a* and 14*b*, net ozone destruction is typically indicated for mt and mm air masses in the middle free troposphere. In contrast, calculated net ozone conversion rates are much more variable in

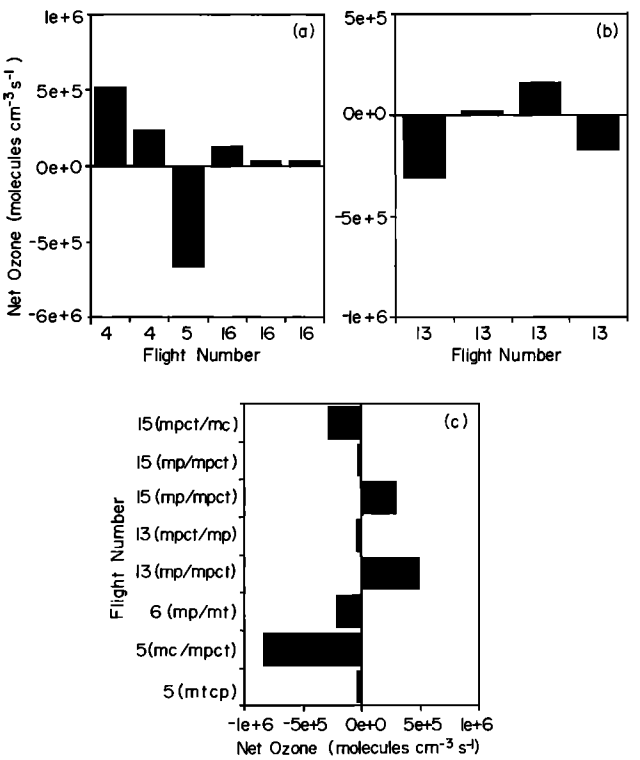

Fig. 15. Calculated net ozone conversion rates, $P(O_3)$, for continental regions at altitudes of ≥4.7 km: (*a*) mixed continental (mc) air masses, (*b*) maritime polar mixed with continental tropical (mpct) air masses, and (*c*) mixtures of the various air mass categories.

mp middle free tropospheric air masses (Figure 14*c*). In this case, there are three instances each of significant O_3 destruction, significant O_3 production, and near balance in net ozone conversion. Overall, of the 24 maritime middle free tropospheric cases examined, significant net ozone production was indicated in only four cases (16.7%), and significant net ozone destruction was indicated in 15 cases (62.5%).

Seventeen continental environments at altitudes of ≥4.7 km were examined with respect to net ozone conversion rates, but not all may be stated to be middle or even lower free tropospheric in nature. While significant net ozone production was indicated in 50% of the mc air mass cases examined (33.3% of the continental cases were categorized as mixed, Figure 15*a*), only three instances (25%) of significant net ozone production were indicated in the remaining continental air mass categories (Figures 15*b* and 15*c*). Indeed, in 33.3% of all of the continental environments considered (altitudes of ≥4.7 km), significant net ozone destruction is indicated, and in a second 33.3% of the data, net ozone conversion is indicated to be nearly in balance. Of the 11 cases examining data obtained at altitudes of <4.7 km (Figure 16), significant positive net ozone production was only indicated in mpct air masses at 2.1 km over the continent during flight 14, in mp air masses at 2.3 km over the ocean during flight 12, and in mp air in the marine boundary layer during flight 10. In the latter case it should be noted that if $P(O_3)$ is recalculated excluding all hydrocarbons, the result indicates net ozone destruction (-3.8 times 10^5 molecules cm^{-3} s^{-1}). (The model was routinely run with and without hydrocarbons, but little difference was typically observed in the calculated net ozone conversion rates. In this case, ambient propylene was measured at 100 pptv, significantly higher

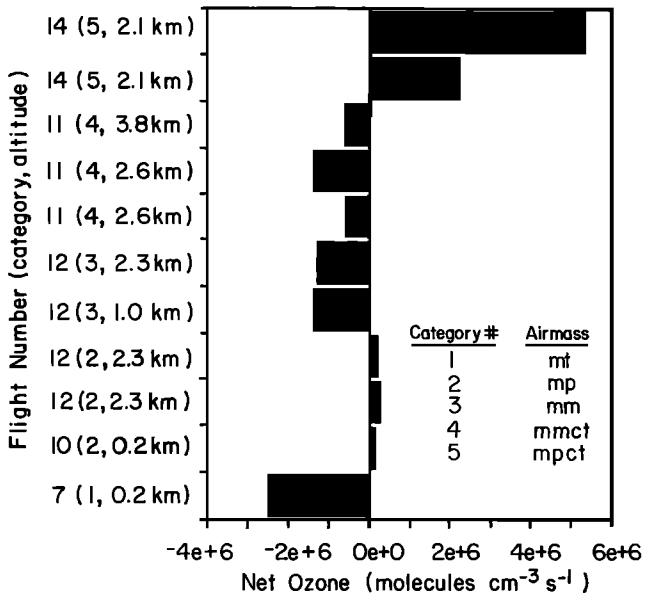

Fig. 16. Calculated net ozone conversion rates, $P(O_3)$, for maritime and continental environments at altitudes of <4.7 km.

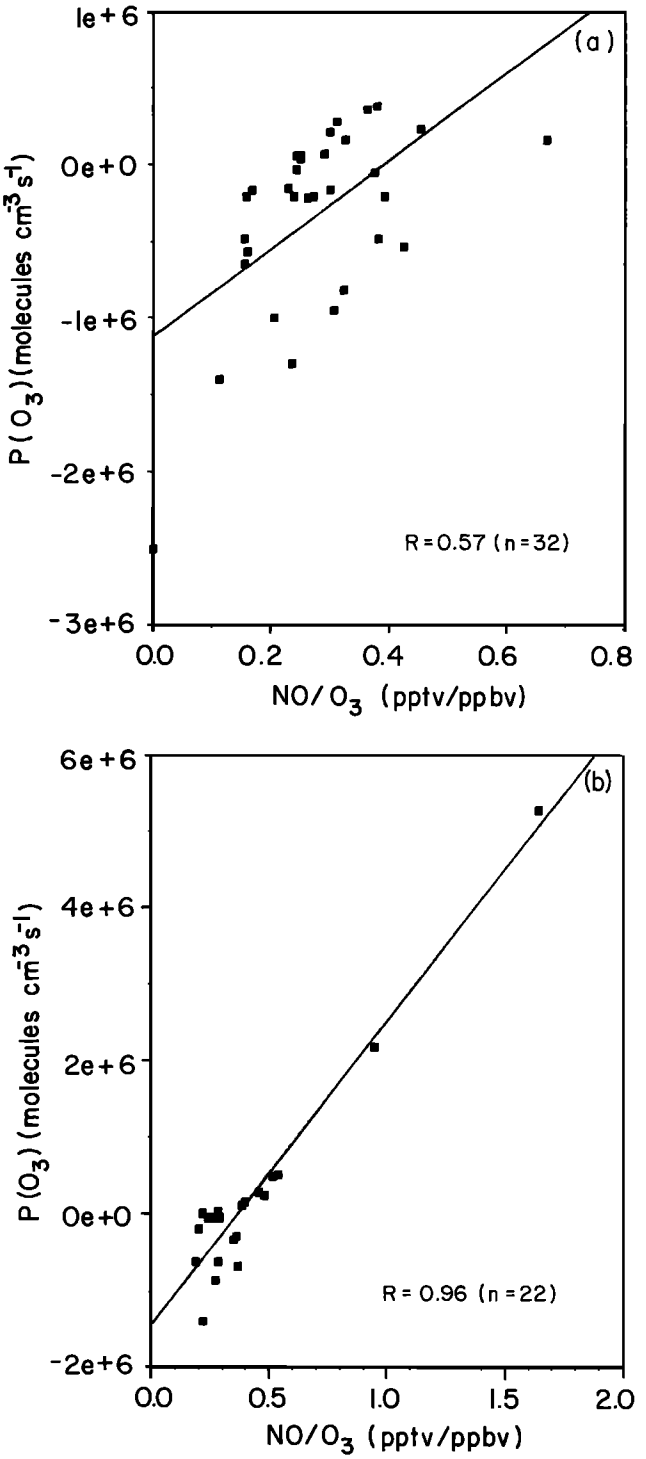

Fig. 17. Calculated net ozone conversion rates, $P(O_3)$, plotted versus the ratio of ambient NO (pptv) to ambient O_3 (ppbv) for (*a*) maritime air masses and (*b*) continental air masses.

than other measurements in this data set (see Table 1).) In all other instances (54.5% of the data), even in mmct air masses, significant net ozone destruction was indicated.

When ambient NO mixing ratios exceed the critical level, net ozone production is expected, while ambient NO mixing ratios less than critical NO are expected to lead to net ozone destruction. As expected, then, a significant

positive correlation is observed between $P(O_3)$ and ambient NO in both maritime and continental air masses. There is a considerable range of NO mixing ratios that result in both net ozone production and loss, signifying that the critical level of NO varies considerably from air mass to air mass, depending upon hydrocarbon, H_2O, O_3, and NO mixing ratios, and is often greater than 10 pptv. In the case of the maritime data, net ozone destruction is always indicated for NO <10 pptv, but net ozone production is not always indicated for NO > 10 pptv. In the continental data, net ozone production is always indicated only for NO mixing ratios of >20 pptv. Plots of $P(O_3)$ versus NO/O_3 (pptv/ppbv) (Figures 17*a* and 17*b*) show similar variability for the maritime data but show a more clear-cut definition for the continental set. In the maritime data (Figure 17*a*), net ozone production is always indicated for $NO/O_3 \leq 0.23$, but $NO/O_3 > 0.23$ results in both ozone production and loss, depending on the air mass. However, in the continental data (Figure 17*b*), net ozone production is always indicated for $NO/O_3 > 0.38$, and a balance or net ozone destruction is always indicated for $NO/O_3 \leq 0.38$. In the spring 1984 CITE 1 data set a clear delineation was also seen; when all of the data were plotted together, $P(O_3) > 0$ for $NO/O_3 > 0.3$ and $P(O_3) < 0$ for $NO/O_3 < 0.3$ [*Ridley et al.*, 1989].

NO_x/NO_y

Total reactive nitrogen was measured simultaneously with NO and NO_2 during GTE/CITE 2, and, as previously mentioned, measurements were also made of the other two major (identified) daytime species, PAN and HNO_3. The distribution of NO_y and the partitioning within the odd nitrogen family are the subject of separate papers (G. Hübler et al., unpublished material, 1990). Only a brief overview of the observed contribution of NO_x to NO_y will be given here. Distribution plots for the ratio of NO_x to NO_y for the maritime and continental data sets are shown in Figure 18. These plots were generated using all NO_x as the time base, since NO_y measurements had a resolution of 10 s and hence the NO_y data set is much larger than the NO_x set. The plots clearly show that NO_x is typically only a small fraction of NO_y in the air masses encountered. The median contribution of NO_x to NO_y was about 11% in maritime air masses and 15% in continental air masses.

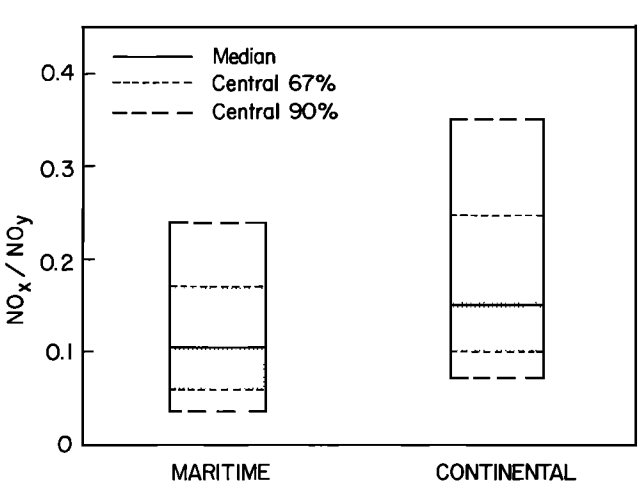

Fig. 18. Distribution plots showing median, central 67% (shaded areas) and central 97% are given for NO_x/NO_y in maritime and continental air masses.

Also shown in Figure 18 are the central 67% and the central 90% of the distribution. It is clear that the variability in the ratio was significantly greater in the continental environments sampled than in the maritime air masses encountered. This is not surprising, given the high variability of the sources over the continent, especially those that introduce fresh NO_x into the atmosphere leading to significantly higher NO_x/NO_y than in, for example, the source-free marine boundary layer.

CONCLUSIONS

Median values of daytime NO and daytime and nighttime NO_2 and NO_x in the marine boundary layer were 4.0, 10.4, and 15.7 pptv, respectively. In the lower free troposphere (1-3 km) in maritime air masses, median mixing ratios were 7.0 pptv NO, 14.2 pptv NO_2, and 20.5 pptv NO_x. For the middle free troposphere (3-6.5 km) in maritime air masses, median daytime NO was 12.4 pptv, and median daytime and nighttime NO_2 and NO_x were 18.0 pptv and 31.0 pptv, respectively. These middle free tropospheric values are similar to those observed during the fall 1983 (NO only) [*Ridley et al.*, 1987] and spring 1984 (NO and NO_2) [*Ridley et al.*, 1989] CITE 1 measurement programs, thus no large seasonal difference is observed for the NO_x species. When considering all of the maritime measurements of O_3 and CO, the median values were 43.5 and 86.0 ppbv, respectively. Average maritime O_3 for CITE 2 (43.1 ± 17.0 ppbv) were similar to those encountered during spring 1984 (48 ± 13 ppbv), and both summer 1986 and spring 1984 average maritime O_3 values are significantly greater than those observed during fall 1983 (27 ± 6 ppbv). In contrast, average maritime CO for CITE 2 (89.2 ± 19.8 ppbv) were similar to those observed during fall 1983 and lower than those observed during spring 1984 (121 ± 11 ppbv).

Median values of daytime NO and daytime and nighttime NO_2 and NO_x in the continen- tal boundary layer (1-3 km) were 34.5, 75.0, and 118.3 pptv, respectively. For coninental air masses at altitudes of 3-6.5 km, median mixing ratios were 13.0 pptv NO, 36.0 pptv NO_2, and 51.0 pptv NO_x. As previously discussed, this data subset includes data obtained in the continental boundary layer and in the free troposphere over the continental southwestern United States; thus it is inappropriate to compare these values with measurements made purely in the continental free troposphere. When considering all of the measurements of O_3 and CO obtained in continental air masses, the median values were 47.5 and 101.0 ppbv, respectively. In comparison with average continental values from spring 1984, summer 1986 average O_3 (47.1 ± 14.5) was slightly higher (42.9 ± 9.4 pptv in spring 1984), and average CO

(101.6 ± 23.6) was lower than spring 1984 average CO (115 ± 21 pptv).

Altitude profiles deduced from the median values stated above indicate a positive gradient with altitude for NO, NO_2, and NO_x in maritime air masses, while the opposite is true in continental air masses. In contrast, altitude profiles obtained in situ are typically highly structured.

Additional contrasts observed include the following: positive correlations between NO_x and DPT were typically observed in continental air masses, while NO_x and DPT showed little or negative correlation in maritime air masses at altitudes of ≥1 km, and, while no significant variability was seen among the data in the maritime air masses, the opposite was true for the continental air mass categories. These differences might be due to the widely differing source regions for the maritime air masses, and the rather arbitrary categorization resulting in a sort of blending or dilution of the air masses having continental influence so that mixtures were more typical than a single air mass type. Furthermore, correlations indicative of fresh pollution sources would be expected in the continental boundary layer, thus the contrast in the correlations between NO_x and DPT in the maritime and continental data sets might be expected. Overall, a positive correlation was typically observed between NO_x and O_3, although the degree of correlation between these species in maritime air masses is significantly higher than that observed in continental air masses. The latter correlation is significantly improved when the highest values of NO_x are not included, as a high degree of correlation between these species is not expected when sampling in environments near fresh sources of pollution where balance between ozone production and destruction has not yet been achieved. It is important to point out that the correlations discussed in this treatment of the data are often not as crisp as those obtained when examining the individual data sets. For example, the data set used in the correlation analyses presented here include all data points submitted as final data by each group, including York $NO_2 < 50$ pptv. Correlations and altitude profiles obtained by examining "average" data sets must be compared with those obtained from the individual sets so that misrepresentations of the data are avoided.

Significant net ozone destruction was indicated in 62.5% of the maritime middle free tropospheric (3-6.5 km) cases examined, and in 33.3% of the continental cases examined (altitudes of ≥4.7 km, though not necessilary free tropospheric). Significant net ozone production was indicated in 33.3% of all of the continental environments considered (altitudes of ≥4.7 km) and in only 16.7% of the cases examined for the maritime middle free troposphere. From this treatment of the data, the middle free troposphere over the eastern Pacific Ocean is expected to be a region of limited NO, or of net ozone destruction. This conclusion agrees with that drawn from measurements made during spring 1984 [*Ridley et al.*, 1989]. It is important to note that while the $P(O_3)$ values were calculated from ambient values of NO, O_3, and so on, obtained within several hours of local noon, daily averages of $P(O_3)$, though smaller, would remain negative.

NO_x typically was a small fraction of NO_y in the air masses encountered during CITE 2. Median values for the maritime and continental air mass categories show that NO_x was only 11% and 15% of NO_y, respectively, although considerably greater variability was observed for the ratio in the continental data set, likely reflecting the widely varying continental environments.

Acknowledgments. We thank R. Navarro, the flight crew, and the maintenance personnel of the NASA Wallops Island Flight Facility responsible for the Electra aircraft. We also thank the personnel at the NASA Ames Research Center for providing facilities for many of the flights and the ground-based operations, and J. M. Hoell, Jr., for project office support. M.A.C. and D.D.M. also thank P. Murphy for his expertise in providing the excellent data collection and analysis software, and C. Eubank for standards calibrations. D.R.H. and H.I.S. also thank A. Taylor and S. Barzetti for data analysis, as well as the Natural Sciences and Engineering Research Council and the Atmospheric Environment Service of Canada for support. Partial support was provided by the NASA Tropospheric Chemistry Program. The National Center for Atmospheric Research is sponsored by the National Science Foundation.

REFERENCES

Chameides, W. L., The photochemical role of tropospheric nitrogen oxides, *Geophys. Res. Lett.*, *5*, 17-20, 1978.

Chameides, W. L., and D. H. Stedman, Tropospheric ozone, coupling transport and photochemistry, *J. Geophys. Res.*, *82*, 1787-1794, 1977.

Chameides, W. L., and J. C. G. Walker, A photochemical theory of tropospheric ozone, *J. Geophys. Res.*, *78*, 8751-8760, 1973.

Chameides, W. L., and J. C. G. Walker, A time-dependent photochemical model for ozone near the ground, *J. Geophys. Res.*, *81*, 413-420, 1976.

Chameides, W.L., D. D. Davis, M. O. Rodgers, J. Bradshaw, S. Sandholm, G. Sachse, G. Hill, G. Gregory, and R. Rasmussen, Net ozone photo-chemical production over the eastern and central North Pacific as inferred from GTE/CITE 1 observations during Fall 1983, *J. Geophys. Res.*, *92*, 2131-2152, 1987.

Chameides, W. L., et al., Observed and model-calculated NO_2/NO ratios in tropospheric air sampled during the NASA GTE/CITE 2 field study, *J. Geophys. Res.*, this issue.

Crutzen, P.J., Photochemical reactions initiated by and influencing ozone in unpolluted troposperic air, *Tellus*, *26*, 47-57, 1974.

Dignon, J. and S. Hameed, A model investigation of the impact of increases in anthropogenic NO_x emissions between 1967 and 1980 on tropospheric ozone, *J. Atmos. Chem.*, *3*, 491-506, 1985.

Fehsenfeld, F. C., et al., Intercomparison of NO_2 measurement techniques, *J. Geophys. Res.*, *95*, 3579-3598, 1990.

Fishman, J., and P. J. Crutzen, A numerical study of tropospheric photochemistry using a one- dimensional model, *J. Geophys. Res.*, *82*, 5897-5906, 1977.

Fishman, J., and P. J. Crutzen, The origin of ozone in the troposphere, *Nature*, *274*, 855-858, 1978.

Fishman, J., V. Ramanathan, P. J. Crutzen, and S. C. Liu, Tropospheric ozone and climate, *Nature, 282*, 818-820, 1979*a*.

Fishman, J., S. Solomon, and P. J. Crutzen, Observational and theoretical evidence in support of a significant in situ photochemical source of tropospheric ozone, *Tellus, 31*, 432-446, 1979*b*.

Gregory, G. L., J. M. Hoell, Jr., A. L. Torres, M. A. Carroll, B. A. Ridley, M. O. Rodgers, J. Bradshaw, S. T. Sandholm, and D. D. Davis, An intercomparison of airborne nitric oxide measurements: A second opportunity, *J. Geophys. Res.*, this issue (*a*).

Gregory G. L., et al., An intercomparison of airborne nitrogen dioxide instruments, *J. Geophys. Res.* , this issue (*b*).

Gregory G. L., et al., An intercomparison of airborne nitric acid measurements, *J. Geophys. Res.* , this issue (*c*).

Gregory G. L., et al., An intercomparison of airborne peroxyacetyl nitrate measurements, *J. Geophys. Res.* , this issue (*d*).

Hastie, D. R., H. I. Schiff, J. D. Bradshaw, D. D. Davis, M. O. Rodgers, S. T. Sandholm, M. A. Carroll, B. A. Ridley, and A. L. Torres, Generating NO_x concentrations from the CITE II NO and NO_2 concentrations (abstract), *Eos Trans. AGU, 68*, 1213, 1987.

Hoell, J. M. Jr., D. L. Albritton, G. L. Gregory, R. J. McNeal, S. M. Beck, R. J. Bendura, and J. W. Drewry, Operational overview of NASA GTE/CITE 2 airborne instrument intercomparisons: Nitrogen dioxide, nitric acid, and peroxyacetyl nitrate, *J. Geophys. Res.*, this issue.

Huebert, B. J.,et al., Measurements of the nitric acid to NO_x ratio in the troposphere, *J. Geophys. Res.*, this issue.

LeBel, P. J., B. J. Huebert, H. I. Schiff, S. A. Vay, S. E. Van Bramer, and D. R. Hastie, Measurements of tropospheric nitric acid over the western United States and northeastern Paciric Ocean, *J. Geophys. Res.*, this issue.

Liu, S. C., Possible effects on tropospheric O_3 and OH due to NO emissions, *Geophys. Res. Lett., 1*, 325-328, 1977.

Liu, S. C., D. Kley, M. McFarland, J. D. Mahlman, and H. Levy, II, On the origin of tropospheric ozone, *J. Geophys Res., 85*, 7546-7552, 1980.

Liu, S. C., M. McFarland, D. Kley, O. Zafiriou, and B. Huebert, Tropospheric NO_x and O_3 budgets in the equatorial Pacific, *J. Geophys. Res., 88*, 1360-1368, 1983.

Liu, S. C., M. Trainer, F. C. Fehsenfeld, D. D. Parrish, E. J. Williams, D. W. Fahey, G. Hübler, and P. C. Murphy, Ozone production in the rural troposphere and the implications for regional and global ozone distributions, *J. Geophys. Res. 92*, 4191-4207, 1987.

Logan, J. A., Nitrogen oxides in the troposphere: Global and regional budgets, *J. Geophys. Res., 88*, 10,785-10,807, 1983.

Logan, J. A., Tropospheric ozone: Seasonal behavior, trends, and anthropogenic influence, *J. Geophys. Res., 90*, 10,463-10,482, 1985.

Logan, J. A., M. J. Prather, S. C. Wofsy, and M. B. McElroy, Tropospheric chemistry: A global perspective, *J. Geophys Res., 86*, 7210-7254, 1981.

Madronich, S., Intercomparison of NO_2 photodissociation and u.v. radiometer measurements, *Atmos. Environ., 21*, 569-578, 1987.

Ridley, B. A., M. A. Carroll, and G. L. Gregory, Measurements of nitric oxide in the boundary layer and free troposphere over the Pacific Ocean, *J. Geophys. Res., 92*, 2025-2047, 1987.

Ridley, B. A., M. A. Carroll, G. L. Gregory, and G. W. Sachse, NO and NO_2 in the troposphere: Technique and measurements in regions of a folded tropopause, *J. Geophys. Res., 93*, 15,813-15,830, 1988*a*.

Ridley, B. A., M. A. Carroll, A. L. Torres, E. P. Condon, G. W. Sachse, and G. L. Gregory, An intercomparison of results from ferrous sulphate and photolytic converter techniques for measurements of NO_x made during the NASA GTE/CITE 1 aircraft program, *J. Geophys. Res., 93*, 15,803-15,811, 1988*b*.

Ridley, B. A., M. A. Carroll, D. D. Dunlap, M. Trainer, G. W. Sachse, G. L. Gregory, and E. P. Condon, Measurements of NO_x over the eastern Pacific Ocean and southwestern United States during the spring 1984 NASA GTE Aircraft Program, *J. Geophys Res., 94*, 5043-5067, 1989.

Ridley, B. A., et al., Ratios of peroxyacetyl nitrate to active nitrogen observed during aircraft flights over the eastern Pacific Ocean and continental United States, *J. Geophys Res.*, this issue.

Sandholm, S. T., J. D. Bradshaw, K. S. Dorris, M. O. Rodgers, and D. D. Davis, An airborne compatible photofragmentation two-photon laser-induced fluorescence instrument for measuring tropospheric NO, NO_X, and NO_2, *J. Geophys Res.*, this issue.

Schiff, H. I., D. R. Karecki, G. W. Harris, D. R. Hastie, and G. I. Mackay, A tunable diode laser system for aircraft measurements of trace gases, *J. Geophys Res.*, this issue.

Shipham, M., A. S. Bachmeier, and D. R. Cahoon, Meteorological conditions during the summer 1986 CITE 2 flight series, *J. Geophys Res.*, this issue.

Singh, H. B., et al., Peroxyacetyl nitrate measure- ments during CITE 2: Atmospheric distribution and precursor relationships, *J. Geophys Res.*, this issue.

Trainer, M., E. Y. Hsie, S. A. McKeen, R. Tallamraju, D. D. Parrish, F. C. Fehsenfeld, and S. C. Liu, Impact of natural hydrocarbons on hydroxyl and peroxy radicals at a remote site, *J. Geophys. Res., 92*, 11,879-11,894, 1987.

D. L. Albritton, M. A. Carroll, G. Hübler, D. D. Montzka, and M. Trainer, National Oceanic and Atmospheric Administration, Aeronomy Laboratory, 325 Broadway, Boulder, CO 80303.

A. S. Bachmeier, Lockheed, Hampton, VA 23665.

S. M. Beck, G. L. Gregory, and M. C. Shipham, NASA Langley Research Center, Hampton, VA 23665.

J. D. Bradshaw, D. D. Davis, M. O. Rodgers, and S. T. Sandholm, School of Geophysical Sciences, Georgia Institute of Technology, Atlanta, GA 30332.

E. P. Condon and H. B. Singh, NASA Ames Research Center, Moffett Field, CA 94035.

G. W. Harris, D. R. Karecki, and G. I. Mackay, Unisearch Associates, Concord, Ontario, Canada L4K 1B5.

D. R. Hastie and H. I. Schiff, Chemistry Department, York University, Downsview, Ontario, Canada.

S. Madronich and B. A. Ridley, National Center for Atmospheric Research, P. O. Box 3000, Boulder, CO 80307.

A. L. Torres, NASA Goddard Space Flight Center, Wallops Flight Facility, Wallops Island, VA 23337.

(Received June 5, 1989;
revised September 12, 1989;
accepted September 13, 1989.)